

1 **Benthic Archaea as potential sources of tetraether membrane**
2 **lipids in sediments across an oxygen minimum zone**

3 Marc A. Besseling^{1*}, Ellen C. Hopmans¹, Jaap S. Sinninghe Damsté^{1,2}, and Laura Villanueva¹

4 ¹NIOZ Royal Netherlands Institute for Sea Research, Department of Marine Microbiology and Biogeochemistry, and
5 Utrecht University. P.O. Box 59, NL-1790 AB Den Burg, The Netherlands.

6 ²Utrecht University, Faculty of Geosciences, Department of Earth sciences, P.O. Box 80.021, 3508 TA Utrecht, The
7 Netherlands

8 *Correspondence to:* Marc A. Besseling (marc.besseling@nioz.nl)

9 **Abstract.** Benthic Archaea comprise a significant part of the total prokaryotic biomass in marine sediments. Recent
10 genomic surveys suggest they are largely involved in anaerobic processing of organic matter but the distribution and
11 abundance of these archaeal groups is still largely unknown. Archaeal membrane lipids composed of isoprenoid
12 diethers or tetraethers (glycerol dibiphytanyl glycerol tetraether, GDGT) are often used as archaeal biomarkers. Here,
13 we compare the archaeal diversity and intact polar lipid (IPL) composition in both surface (0–0.5 cm) and subsurface
14 (10–12 cm) sediments recovered within, just below, and well below the oxygen minimum zone (OMZ) of the Arabian
15 Sea. Archaeal 16S rRNA gene amplicon sequencing revealed a predominance of Thaumarchaeota (Marine Group I,
16 MG-I) in oxygenated sediments. Quantification of archaeal 16S rRNA and ammonia monooxygenase (*amoA*) of
17 Thaumarchaeota genes and their transcripts indicated the presence of an active *in situ* benthic population, which
18 coincided with a high relative abundance of hexose phosphohexose crenarchaeol, a specific biomarker for living
19 Thaumarchaeota. On the other hand, anoxic surface sediments within the OMZ and all subsurface sediments were
20 dominated by archaea belonging to the Miscellaneous Crenarchaeota Group (MCG), the Thermoplasmatales and
21 archaea of the DPANN superphylum. Members of the MCG were diverse with a dominance of subgroup MCG-12 in
22 anoxic surface sediments. This coincided with a high relative abundance of IPL GDGT-0 with an unknown polar head
23 group. Subsurface anoxic sediments were characterized by higher relative abundance of GDGT-0, 2 and 3 with
24 dihexose IPL-types, as well as GDGT-0 with a cyclopentanetetraol molecule and a hexose, as well as the presence of
25 specific MCG subgroups, suggesting that these groups could be the biological sources of these archaeal lipids.

26 INTRODUCTION

27 Archaea are ubiquitous microorganisms in the marine system (DeLong et al., 1994; Delong and Pace, 2001; Schleper et
28 al., 2005). They occur in diverse environments, e.g. hydrothermal vents (Stetter et al., 1990), the marine water column
29 (Karner et al., 2001; Massana et al., 2004), in the underlying sediments (Lloyd et al., 2013; Teske and Sørensen, 2008),
30 and well below the seafloor (Biddle et al., 2006; Lipp et al., 2008), where they are considered key players in diverse
31 biogeochemical processes (Offre et al., 2013, and references cited therein). Specifically marine sediments have been
32 shown to contain a highly diverse archaeal community (Lloyd et al., 2013; Spang et al., 2017; Teske, 2013; Teske and
33 Sørensen, 2008). The ammonia-oxidizing Thaumarchaeota of the marine group I.1a (further referred to as MG-I) is
34 probably the most widely studied archaeal group in marine sediments. However, in comparison with studies of marine
35 pelagic Thaumarchaeota, the diversity and distribution of benthic Thaumarchaeota is still not well established (e.g.
36 Durbin & Teske, 2010; Jorgenson et al., 2012; Learman et al., 2016). Genomic studies have revealed the existence of
37 uncultured archaeal groups other than Thaumarchaeota in marine, predominantly anoxic, sediments such as the
38 Miscellaneous Crenarchaeota Group (MCG; Meng et al., 2014), archaea of the DPANN superphylum (composed of
39 Micrarchaeota, Diapherotrites, Aenigmarchaeota, Nanohaloarchaeota, Parvarchaeota, Nanoarchaeota, Pacearchaeota
40 and Woearchaeota; Castelle et al., 2015; Rinke et al., 2013) and the Marine Benthic Group (MBG) B (Teske &
41 Sørensen, 2008), and D (Lloyd et al., 2013). In the case of the archaea belonging to the groups of the MCG and MBG-
42 D, metagenomic studies suggest that they are able to degrade extracellular proteins and aromatic compounds (Lloyd et
43 al., 2013; Meng et al., 2014).

44 Archaeal diversity is currently determined through nucleic acid-based methods but the characterization of other cellular
45 biomarkers such as membrane lipids has proven to be also effective in tracking the presence of archaeal groups in
46 different ecosystems (e.g. Coolen et al., 2004a; Ingalls et al., 2012; Meador et al., 2015; Pitcher et al., 2011b; Sturt et
47 al., 2004). One of the advantages of using lipid-based methods to determine the presence of archaeal groups is that
48 lipids can be preserved in the sedimentary record. Therefore, they can also be used as biomarkers of the presence and
49 metabolic potential of these microorganisms in past environments. On the contrary, other biomolecules like DNA have
50 a more rapid turnover and they cannot be used for this purpose. In recent years, intact polar lipids (IPLs) have
51 increasingly been applied for tracing 'living' bacteria and archaea in the environment (Lipp et al., 2008; Lipp and
52 Hinrichs, 2009; Rossel et al., 2008). IPLs with polar head groups are present in living cells but upon cell lysis the polar
53 head groups are lost, releasing core lipids (CLs) that may be preserved in the fossil record. Since IPLs degrade
54 relatively quickly after cell death (Harvey et al., 1986), it is possible to associate the presence of IPLs in the
55 environment with the occurrence of their living producers (Lipp and Hinrichs, 2009; Schubotz et al., 2009).

56 Archaeal membrane lipids are typically a variation of two main structures, *sn*-2,3-diphytanylglycerol diether (archaeol)
57 with phytanyl (C₂₀) chains in a bilayer structure, and *sn*-2,3-dibiphytanyl diglycerol tetraether (glycerol dibiphytanyl
58 glycerol tetraether, GDGT), in which the two glycerol moieties are connected by two C₄₀ isoprenoid chains, allowing

59 the formation of a monolayer membrane (Koga and Morii, 2007). GDGTs containing 0–4 cyclopentane moieties (Fig.
60 S1) are usually not exclusive to a specific archaeal group (Schouten et al., 2013) with the exception of the GDGT
61 crenarchaeol, containing 4 cyclopentane and one cyclohexane moiety, which is deemed to be exclusive to the
62 Thaumarchaeota phylum (De La Torre et al., 2008; Sinninghe Damsté et al., 2002, 2012). Recently, Lincoln et al.
63 (2014) proposed the Marine Group II as potential producers of crenarchaeol. However, this is still debated (Lincoln et
64 al., 2014b; Schouten et al., 2014). The newly described archaeal groups detected by genetic methods are yet uncultured,
65 therefore, their membrane lipid composition remains unknown.

66 In this study, we determined the archaeal diversity in a marine benthic system along a strong gradient in bottom water
67 oxygen concentrations and compared it with the diversity of archaeal lipids. We aimed to characterize changes in the
68 archaeal benthic community under different physicochemical conditions, as well as to provide clues on the potential
69 archaeal lipid biomarkers produced by uncultured benthic archaea. We analyzed sediments (surface 0–0.5 cm, and
70 subsurface 10–12 cm) of the Murray ridge in the Arabian Sea, which is impinged by one of the strongest present-day
71 oxygen minimum zones (OMZ). Previous studies observed changes in the diversity of archaeal lipids in the same
72 environmental setting in sediments under different oxygen and nutrient concentrations (Lengger et al., 2012; 2014). In
73 our study, we expand the repertoire of archaeal lipid diversity previously detected by Lengger et al. (2012; 2014) by
74 analyzing these sediments with High Resolution Accurate Mass/Mass spectrometry (UHPLC-HRAM MS). In addition,
75 we determined the archaeal diversity by means of 16S rRNA gene amplicon sequencing, as well as the abundance and
76 potential activity of specific archaeal groups by quantitative PCR (QPCR) of 16S rRNA and the metabolic gene coding
77 for the ammonia monooxygenase (*amoA* gene) of Thaumarchaeota.

78 **MATERIAL and METHODS**

79 **Sampling**

80 Sediments were collected in the Northern Arabian Sea during the PASOM cruise in January 2009 with *R/V Pelagia*.
81 Sediment cores obtained with a multicorer were taken on the Murray ridge at four depths, 885 m below sea level (mbsl)
82 (within the OMZ), at 1306 mbsl (just below the OMZ), at 2470 mbsl and 3003 mbsl (both well below the OMZ) as
83 previously described by Lengger et al. (2012). Upon retrieval the cores were sliced in 0.5 cm resolution for the first 2
84 cm and at 2 cm resolution beyond 10 cm below the surface, and stored at -80°C until further analysis. For an overview
85 of the surface sediments physicochemical conditions see Table 1.

86 **Lipid extraction and analysis**

87 Total lipids were extracted from surface (upper 0–0.5 cm) and subsurface (10–12 cm) sediments after freeze-drying
88 using a modified Bligh and Dyer method (Bligh and Dyer, 1959) as previously described by Lengger et al. (2014). C₁₆-
89 PAF (1-O-hexadecyl-2-acetyl-sn-glycero-3-phosphocholine) was added to the extracts as an internal standard and the

90 extracts were dried under a stream of nitrogen. The extracts with the added standard were then dissolved by adding
91 solvent (hexane:isopropanol:H₂O 718:271:10 [v/v/v/v]) and filtered through a 0.45 µm, 4 mm-diameter True
92 Regenerated Cellulose syringe filter (Grace Davison, Columbia, MD, USA).

93 IPLs were analyzed according to Sturt et al. (2004) with some modifications. An Ultimate 3000 RS UHPLC, equipped
94 with thermostated auto-injector and column oven, coupled to a Q Exactive Orbitrap MS with Ion Max source with
95 heated electrospray ionization (HESI) probe (Thermo Fisher Scientific, Waltham, MA), was used. Separation was
96 achieved on a YMC-Triart Diol-HILIC column (250 x 2.0 mm, 1.9 µm particles, pore size 12 nm; YMC Co., Ltd,
97 Kyoto, Japan) maintained at 30 °C. The following elution program was used with a flow rate of 0.2 mL min⁻¹: 100% A
98 for 5 min, followed by a linear gradient to 66% A: 34% B in 20 min, maintained for 15 min, followed by a linear
99 gradient to 40% A: 60% B in 15 min, followed by a linear gradient to 30% A: 70% B in 10 min, where A = hexane/2-
100 propanol/formic acid/14.8 M NH_{3aq} (79:20:0.12:0.04 [v/v/v/v]) and B = 2-propanol/water/formic acid/ 14.8 M NH_{3aq}
101 (88:10:0.12:0.04 [v/v/v/v]). Total run time was 70 min with a re-equilibration period of 20 min in between runs. HESI
102 settings were as follows: sheath gas (N₂) pressure 35 (arbitrary units), auxiliary gas (N₂) pressure 10 (arbitrary units),
103 auxiliary gas (N₂) T 50 °C, sweep gas (N₂) pressure 10 (arbitrary units), spray voltage 4.0 kV (positive ion ESI),
104 capillary temperature 275 °C, S-Lens 70 V. IPLs were analyzed with a mass range of *m/z* 375 to 2000 (resolving power
105 70,000 at *m/z* 200), followed by data dependent MS² (resolving power 17,500 ppm at *m/z* 200), in which the ten most
106 abundant masses in the mass spectrum (with the exclusion of isotope peaks) were fragmented (stepped normalized
107 collision energy 15, 22.5, 30; isolation window 1.0 *m/z*). A dynamic exclusion window of 6 sec was used as well as an
108 inclusion list with a mass tolerance of 3 ppm to target specific compounds (Table S1). The Q Exactive Orbitrap MS was
109 calibrated within a mass accuracy range of 1 ppm using the Thermo Scientific Pierce LTQ Velos ESI Positive Ion
110 Calibration Solution (containing a mixture of caffeine, MRFA, Ultramark 1621, and *N*-butylamine in an acetonitrile-
111 methanol-acetic acid solution).

112 Peak areas for each individual IPL were determined by integrating the combined mass chromatogram (within 3 ppm) of
113 the monoisotopic and first isotope peak of all relevant adducts formed (protonated, ammoniated and/or sodiated adducts
114 may be formed in different proportions depending on the type of IPL). PAF was used as internal standard to
115 continuously monitor MS performance and to assess matrix effects. Reported peak areas have been corrected for these
116 effects. Absolute quantification of IPL GDGTs was not possible due to a lack of standards. Peak areas were not
117 corrected for any possible differences in response factors between the various classes of IPL-crenarchaeol. IPLs with
118 the same headgroup but with the regioisomer of crenarchaeol instead of crenarchaeol as the CL co-elute on the
119 chromatographic system used here and any peak area reported for a crenarchaeol IPL thus represents the sum of both
120 isomers.

121 To rule out any degradation of the GDGT-IPLs during storage of the sediments at -20°C, the anoxic surface sediment
122 sample at 885 mbsl was also analyzed according to the method previously used by Lengger et al. (2012). The IPL

123 fraction was separated from the CLs with the use of a silica column and elution with MeOH (Lengger et al., 2012). This
124 IPL fraction was hydrolyzed for 3 h and analyzed by HPLC-APCI/MS (according to Hopmans et al., 2016) and the IPL
125 derived CL-GDGT distribution was compared with previously published data.

126 **Nucleic acids extraction, cDNA synthesis and quantitative PCR (QPCR) analyses**

127 Sediment was centrifuged and the excess of water was removed by pipetting before proceeding with the extraction of
128 nucleic acids from the sediment. DNA/RNA of surface (0–0.5 cm) and subsurface (10–12 cm) sediments was extracted
129 with the RNA PowerSoil® Total Isolation Kit plus the DNA elution accessory (Mo Bio Laboratories, Carlsbad, CA).
130 Concentration of DNA and RNA were quantified by Nanodrop (Thermo Scientific, Waltham, MA) and Fluorometric
131 with Quant-iT™ PicoGreen® dsDNA Assay Kit (Life technologies, Netherlands). RNA extracts were treated with
132 DNase and reverse-transcribed to cDNA as described by Pitcher et al. (2011). Quantification of archaeal 16S rRNA
133 gene copies and *amoA* gene copies were estimated by QPCR by using the following primers; Parch519F and ARC915R
134 (archaeal 16S rRNA gene), CrenAmoAQ-F and CrenAmoAModR (*amoA* gene), as previously described (Pitcher et al.,
135 2011). For details on the QPCR conditions, efficiency and R^2 of the QPCR assays see Table S2.

136 **16S rRNA gene amplicon sequencing, analysis, and phylogeny**

137 PCR reactions were performed with the universal, Bacteria and Archaea, primers S-D-Arch-0159-a-S-15 and S-D-Bact-
138 785-a-A-21 (Klindworth et al., 2013) as previously described in Moore et al. (2015). The archaeal 16S rRNA gene
139 amplicon sequences were analyzed by QIIME v1.9 (Caporaso et al., 2010). Raw sequences were demultiplexed and
140 then quality-filtered with a minimum quality score of 25, length between 250–350, and allowing maximum two errors
141 in the barcode sequence. Taxonomy was assigned based on blast and the SILVA database version 123 (Altschul et al.,
142 1990; Quast et al., 2013). Representative operational taxonomic units (OTUs, clusters of reads with 97% similarity) of
143 archaeal groups were extracted through filter_taxa_from_otu_table.py and filter_fasta.py with QIIME (Caporaso et al.,
144 2010). The phylogenetic affiliation of the partial archaeal 16S rRNA gene sequences was compared to release 123 of
145 the Silva NR SSU Ref database (<http://www.arb-silva.de/>; Quast et al., 2013) using the ARB software package (Ludwig
146 et al., 2004). Sequences were added to the reference tree supplied by the Silva database using the ARB Parsimony tool.
147 MCG intragroup phylogeny for representative sequences of OTUs affiliated to the MCG lineage was carried out in
148 ARB (Ludwig et al., 2004). Sequences were added by parsimony to a previously-built phylogenetic tree composed of
149 reference sequences of the 17 MCG subgroups known so far (Kubo et al., 2012). Affiliation of any 16S rRNA gene
150 sequences to a given subgroup was done assuming a similarity cutoff of $\geq 85\%$.

151 **Cloning, sequencing and phylogeny of the archaeal *amoA* gene**

152 Amplification of the archaeal *amoA* gene was performed as described by Yakimov et al., (2011). PCR reaction mixture
153 was the following (final concentration): Q-solution 1× (PCR additive, Qiagen); PCR buffer 1×; BSA (200 $\mu\text{g ml}^{-1}$);
154 dNTPs (20 μM); primers (0.2 $\text{pmol } \mu\text{l}^{-1}$); MgCl_2 (1.5 mM); 1.25 U Taq polymerase (Qiagen, Valencia, CA, USA). PCR

155 conditions for these amplifications were the following: 95°C, 5 min; 35 × [95°C, 1 min; 55°C, 1 min; 72°C, 1 min];
156 final extension 72°C, 5 min. PCR products were gel purified (QIAquick gel purification kit, Qiagen) and cloned in the
157 TOPO-TA cloning® kit from Invitrogen (Carlsbad, CA, USA) and transformed in *E. coli* TOP10 cells following the
158 manufacturer's recommendations. Recombinant clones plasmid DNAs were purified by Qiagen Miniprep kit and
159 screening by sequencing (n ≥ 30) using M13R primer by Macrogen Europe Inc. (Amsterdam, The Netherlands).
160 Obtained archaeal *amoA* protein sequences were aligned with already annotated *amoA* sequences by using the Muscle
161 application (Edgar, 2004). Phylogenetic trees were constructed with the Neighbor-Joining method (Saitou and Nei,
162 1987) and evolutionary distances computed using the Poisson correction method with a bootstrap test of 1,000
163 replicates.

164 **RESULTS**

165 In this study, we analyzed both IPLs and DNA/RNA extracts from sediments previously collected along the Arabian
166 Sea Murray Ridge within the OMZ (885 mbsl), just below the lower interface (1306 mbsl), and well below the OMZ
167 (2470 and 3003 mbsl). The surface sediment (0-0.5 cm) at 885 mbsl was fully anoxic, however, the surface sediments
168 below the OMZ were partly oxygenated (1306 mbsl), and fully oxygenated at 2470 and 3003 mbsl (Table 1). The
169 subsurface sediments (10-12 cm) were fully anoxic at all stations (Table 1). For more details on the physicochemical
170 conditions in these sediments see Table 1.

171 **Archaeal IPL-GDGTs in the surface and subsurface sediments**

172 A range of IPL-GDGTs (GDGT-0 to 4 and crenarchaeol) with the IPL-types monohexose (MH), dihexose (DH) and
173 hexose-phosphohexose (HPH) was detected in surface and subsurface sediments across the Arabian Sea OMZ (Table
174 2). For the DH GDGT-0 two structural isomers (type-I with two hexose moieties at both ends of the CL, and type-II
175 with one dihexose moiety; Table 2) were detected and identified based on their mass spectral characteristics (Fig. S2).
176 These isomers were previously also reported in thaumarchaeotal cultures (Elling et al., 2014, 2017). In addition,
177 GDGT-0 with both an ether-bound cyclopentanetetraol moiety and a hexose moiety as head groups was identified (Fig.
178 S2) in some sediments (Table 2). This IPL was previously reported as a glycerol dibiphytanyl nonitol tetraether
179 (GDNT; de Rosa et al. 1983) but was later shown to contain a 2-hydroxymethyl-1-(2,3-dihydroxypropoxy)-2,3,4,5-
180 cyclopentanetetraol moiety by Sugai et al., (1995) on the basis of NMR spectroscopy characterization.

181 In the surface sediment at 885 mbsl, crenarchaeol IPLs were dominant (44.7% of all detected IPL-GDGTs), occurring
182 predominantly with DH as IPL-type (with a hexose head group on both ends; 43.1%; Table 2). IPL-GDGT-2 was the
183 second most abundant (29.6%), also mainly consisting of the IPL-type DH (29.5%; Table 2). IPL-GDGT-0, -1, -3 and -
184 4 were occurring with relative abundances of 0.3%, 1.7%, 17.8% and 6.1%, respectively (Table 2). Overall, the

185 majority (98.1%; Table 3) of IPL-GDGTs in surface sediment at 885 mbsl with IPL-type DH (all with a hexose
186 molecule on both ends of the CL).

187 The surface sediment at 1306 mbsl contained mostly IPL-GDGT-0 (37.6% of all detected IPL-GDGTs), almost entirely
188 with the IPL-type HPH (36.6% of the total; Table 2). Slightly less abundant was the IPL-crenarchaeol (35.6%), with the
189 IPL-types HPH (18.7%) and DH type-I (15.5%) in equal amounts and with a minor relative abundance with MH
190 (1.4%). Overall, the IPL-GDGTs in surface sediment at 1306 mbsl mainly contained the IPL-types HPH (55.4%; Table
191 3) and DH (42.0%; Table 3).

192 Well below the OMZ, surface sediments from 2470 and 3003 mbsl were both dominated by IPL-GDGT-0 (71.9 and
193 80.8% of all detected IPL-GDGTs, respectively), predominantly with IPL-type HPH (Table 2; Fig. 1a). The IPL-
194 crenarchaeol had a lower relative abundance (26.6 and 17.6%, respectively) and again was dominated by the member
195 with IPL-type HPH (Table 2). The other IPL-GDGTs occurred in minor quantities (<1%). Overall, IPL-type HPH was,
196 thus, by far the most abundant head group detected in surface sediments at 2470 and 3003 mbsl (97.7% and 97.4%,
197 respectively), in contrast to the other two surface sediments studied (Table 3).

198 In all subsurface (10-12 cm) sediments (i.e. at 885, 1306, 2470 and 3003 mbsl) the most abundant IPL-GDGTs were
199 DH-crenarchaeol ($28.9\pm 3.8\%$; Table 2) and DH-GDGT-2 ($25.5\pm 3.5\%$; Table 2). DH was also the most commonly
200 observed IPL-type attached to GDGT-3 and GDGT-4 (Table 2). Overall the distributions of the IPL-GDGTs in all
201 subsurface sediments were relatively similar (Fig. 1a) in comparison to the substantial changes observed at the surface
202 (cf. Fig. 1a). Overall, the IPL-type DH was the predominant one detected in subsurface sediment with a relative
203 abundance ranging from 68.8% at 3003 mbsl to 92.9% at 885 mbsl (Table 3). In contrast to all other sediments, in the
204 subsurface sediments at 885 mbsl and 1306 mbsl, two different isomers (Fig. S2) of the DH-GDGT-0 were detected
205 (Table 2). DH type-I (0.9% at 1306 mbsl) is also found in the other surface and subsurface sediments and in
206 combination with other core GDGT structures, whereas the other isomer (DH type-II) only occurs (7.8% at 885 mbsl;
207 1.8% at 1306 mbsl; Table 2; Fig. S2b). In addition, these subsurface sediments also contain small amounts of GDGT-0
208 with cyclopentanetetraol and MH head groups (IPL-type HCP; 1.6% at 885 mbsl; 0.4% at 1306 mbsl; Table 2; Fig.
209 S2c).

210 We also determined the IPL-derived CL-GDGTs in the 885 mbsl surface sediment following the method of Lengger et
211 al. (2012), in order to exclude IPL degradation within the stored samples. The CL-GDGTs composition derived from
212 freshly obtained IPL showed the same distribution ($r=0.99$, $p < 0.001$) as reported previously (Lengger et al., 2012).

213

214 **Archaeal diversity in the surface and subsurface sediment**

215 Different archaeal groups were detected in surface and subsurface sediment across the Arabian sea OMZ. The surface
216 sediment at 885 mbsl, contained archaeal 16S rRNA gene sequences that were assigned to several archaeal groups (Fig.
217 1b). The most dominant group was MCG (Total 30.5%, 12.2% attributed to C3; also known as MCG-15, Kubo et al.,

218 2012). Another major group found was the DPANN Woesearchaeota Deep sea Hydrothermal Vent Group 6 (DHVEG-
219 6, 20.3%; Fig. 1b; Castelle et al., 2015). Marine Benthic Group (MBG) -B, -D and -E were also present with 12.2%,
220 7.7% and 6.9% of the archaeal 16S rRNA gene reads, respectively (Fig. 1b). Sequences affiliated to the Marine
221 Hydrothermal Vent Group (MHVG, 8.1%) of the phylum Euryarchaeota were also detected (Fig. 1b). Other groups,
222 with lower relative abundances, were Thermoplasmatales groups ANT06-05 (5.7%) and F2apm1A36 (3.3%) and the
223 DPANN Aenigmarchaeota (previously named Deep Sea Euryarchaeotic Group, DSEG; 1.6%; Fig. 1b).

224 Below the OMZ, in partly and fully oxygenated surface sediments at 1306, 2470 and 3003 mbsl (Table 1), the most
225 dominant archaeal group was Thaumarchaeota MG-I with relative abundances of 81.5%, 89.7% and 100%, respectively
226 (Fig. 1b). At 1306 mbsl other archaeal groups, such as MHVG (5.6%), Thermoplasmatales ASC21 (3.2%), DHVEG-6
227 (2.9%), MBG-B (2.4%) and MCG (1.3%) made up the rest of the archaeal community (Fig. 1b). At 2470 mbsl
228 DHVEG-6 (1.1%) was still detectable besides the MG-I (Fig. 1b).

229 In the subsurface sediments (10–12 cm), only the DNA extracted from the sediments at 885 and 1306 mbsl gave a
230 positive amplification signal. The archaeal composition of the subsurface (10–12 cm) sediments at 885 mbsl and 1306
231 mbsl was similar (Fig. 1b; Pearson correlation coefficient of 0.95), with most of the 16S rRNA gene reads classified
232 within the MCG (47.5% and 48.4%, respectively). Other archaeal groups, such as MBG-D (14.4% and 5.7%,
233 respectively), MBG-B (10.1% and 4.4%), the Woesearchaeota (7.8% and 10.4%), were also detected with comparable
234 relative abundances (Fig. 1b). Other archaeal groups such as Thaumarchaeota Terrestrial hot spring, the Euryarchaeota
235 MHVG, MBG-E and the Aenigmarchaeota were detected but at low (< 10%) relative abundance (Fig. 1b). Only minor
236 amount of reads were classified as Thaumarchaeota MG-I (0.5% at 1306 mbsl) (Fig. 1b).

237 Considering the high relative abundance of the MCG detected in the surface sediment at 885 mbsl, as well as in the
238 subsurface (10–12 cm) sediments at 885 mbsl and 1306 mbsl (between 30.5–48.4% of total archaeal 16S rRNA gene
239 reads detected in those samples), we performed phylogenetic analyses to determine the diversity of subgroups of the
240 MCG within these sediments. A total of 57 representative 16S rRNA gene reads assigned to MCG were extracted from
241 the dataset and incorporated in a MCG phylogenetic tree of Fillol et al. (2015) (Fig. 2). The majority of MCG 16S
242 rRNA gene reads from the 885 mbsl surface sediment (77.3%; Table 4) clustered in subgroup 15. In the 885 mbsl
243 subsurface sediment, the majority of MCG reads clustered within subgroups 8 and 15 (33.6% and 19.6%, respectively;
244 Table 4). In the 1306 mbsl surface sediment there was only a low relative abundance of MCG (Fig. 1b); all MCG
245 archaea detected clustered in subgroup 15 (Table 4). On the other hand, in the 1306 mbsl subsurface sediment the reads
246 clustered in subgroups 15, 2 and 14 (34.3%, 10.9% and 10.9%, respectively; Fig. 2).

247 As the Thaumarchaeota MGI was dominant in oxygenated sediments at 1306, 2470 and 3003 mbsl (Fig. 1b), we further
248 analyzed the diversity of this group by performing a more detailed phylogeny of the recovered 16S rRNA gene reads
249 attributed to this group. Five OTUs dominated the Thaumarchaeota MG1 (Table 5); we will refer to them as OTU-1 to -

250 5. OTU-1, 2, 3 and 5 were phylogenetically closely related to other known benthic Thaumarchaeota MGI species, such
251 as ‘*Ca. Nitrosoarchaeum koreensis* MY1’ or environmental 16S rRNA gene sequences from marine sediments (Fig.3).
252 On the other hand, OTU-4 clustered with 16S rRNA gene sequences from pelagic Thaumarchaeota MGI species, like
253 *Ca. Nitrosopelagicus brevis*, and also clustered with 16S rRNA sequences recovered from seawater SPM (Fig. 3).
254 OTU-3 was the most abundant OTU in the surface sediment at 1306, 2470, and 3003 mbsl with a relative abundance of
255 44-68% (Table 5). At 1306 mbsl OTU-4 was the second most abundant (35.1%). This OTU had a much lower relative
256 abundance (1.6% and 0.0%) at 2470 and 3003 mbsl, respectively (Table 5). The relative abundance of OTU-2 increased
257 with increasing sampling station depth (Table 5), OTU-1 and 5 had an abundance <5% in the surface sediments (Table
258 5).

259 The diversity of Thaumarchaeota MG1 was further assessed by amplification, cloning and sequencing of the archaeal
260 *amoA* gene. Most of the *amoA* gene sequences from surface (27 out of 29 clones) and subsurface sediment at 885 mbsl
261 (9 out of 10 clones) and just one from the surface sediment from 1306 mbsl (1 out of 58 clones) were closely related
262 with *amoA* gene sequences previously recovered from SPM at 1050 mbsl from this area of the Arabian Sea (Villanueva
263 et al., 2014). Phylogenetically they fall within the ‘Water column B, subsurface water’ *amoA* clade as defined by
264 Francis et al. (2005) (Fig. 4). At 1306 and 3003 mbsl (surface and subsurface) the majority of recovered *amoA* gene
265 sequences clustered within the ‘shallow water/sediment’ clade (100 and 98.3%, respectively) and are closely related
266 with *amoA* gene sequences from water column SPM at 170 mbsl (Villanueva et al., 2014) as well as *amoA* gene coding
267 sequences previously detected in sediments (Villanueva et al., 2014; Fig. 4). Of all recovered *amoA* gene sequences
268 from 885 mbsl only a small fraction (8.3%) clustered within the ‘shallow water/sediment’ clade (Fig. 4).

269 **Abundance and potential activity of archaea in surface and subsurface sediments**

270 The abundance of archaeal 16S rRNA gene copies in the surface sediments of different stations varied slightly: it was
271 lowest at 1306 mbsl (9.8×10^9 copies g^{-1} sediment) and highest at 2470 mbsl (1.5×10^{11} ; Fig. 5a). The potential
272 activity, based on the 16S rRNA gene transcripts of the archaeal 16S rRNA gene, was the lowest at 2470 mbsl (5×10^4
273 transcripts g^{-1} sediment), while a higher potential activity was detected at 885, 1306 and 3003 mbsl ($0.9-42 \times 10^7$; Fig.
274 5a). The abundance of archaeal 16S rRNA gene copies in the subsurface sediment varied also within one and a half
275 order of magnitude ($1.1-54 \times 10^9$; Fig. 5c), with a decrease with increasing water depth. The potential activity showed
276 less variation within the subsurface sediments ($1.2-22 \times 10^7$ 16S rRNA gene transcripts g^{-1} of sediment; Fig. 5c) than in
277 the surface sediments.

278 The abundance of Thaumarchaeota was estimated by quantifying the archaeal *amoA* gene copies. The highest
279 abundance of *amoA* gene copies in surface sediment was detected at 2470 mbsl (1.0×10^9 copies g^{-1} sediment), and the
280 lowest at 885 mbsl (5×10^4 ; Fig. 5b). *AmoA* gene transcripts in surface sediment were under the detection limit at 885
281 mbsl but were detected below the OMZ with 4×10^2 , 2.3×10^6 and 8×10^3 gene transcripts g^{-1} of sediment at 1306,
282 2470 and 3003 mbsl, respectively (Fig. 5b). In subsurface sediments, the abundance of *amoA* gene copies was low at

283 885 and 1306 mbsl ($5.4\text{-}19 \times 10^2$ gene transcripts g^{-1} sediment) and higher at 2470 and 3003 mbsl (4.1×10^5 , 5.4×10^6 ,
284 respectively; Fig. 5d). *AmoA* gene transcripts were not detected in the subsurface sediments (Fig. 5d).

285 **DISCUSSION**

286 In this study, we assessed the changes in benthic archaeal diversity and abundance in sediments of the Arabian Sea
287 oxygen minimum zone along a gradient in bottom water oxygen concentrations. The steep Murray Ridge protrudes the
288 OMZ, allowing the study of sediments deposited under varying bottom water oxygen concentrations. All these
289 sediments receive organic matter (OM), the most important fuel for benthic prokaryotic activity in sediments. This OM
290 is produced in a relatively small area of the ocean (i.e. the station within the OMZ, at 885 mbsl, and well below the
291 OMZ, at 3003 mbsl, are only 110 km apart) and, therefore, likely composed of the same primary photosynthate.
292 However, due to differences in the degree of mineralization resulting from different exposure to oxic conditions in the
293 water column, there were differences in OM quality. OM in the sediments within the OMZ has a higher biochemical
294 “quality” based on amino acid composition and intact phytopigments compared to OM in the sediments below the OMZ
295 (Koho et al., 2013). Therefore, changes in the quality and flux of OM received by the different sediment niches could
296 also affect the archaeal community composition as several of the archaeal groups (i.e. MCG and MBG-D) reported here
297 have been suggested to use OM as carbon source in anoxic conditions (Lloyd et al., 2013).

298 **Effect of oxygen availability on archaeal diversity and abundance in the surface sediments**

299 We detected large differences in archaeal diversity between the surface sediment deposited within the OMZ and those
300 deposited below the OMZ. In contrast to the diverse anaerobic archaeal community in the surface of 885 mbsl, in
301 surface sediments at 1306, 2470 and 3003 mbsl, Thaumarchaeota MGI were dominant, representing 80-100% of the
302 archaeal population (Fig. 1). This clear difference in the benthic archaeal population in the surface sediments can be
303 attributed to the oxygen availability as Thaumarchaeota are known to require oxygen for their metabolism (i.e.
304 nitrification; Könneke et al., 2005). In fact, the oxygen penetration depth (OPD) was observed to be 3, 10, and 19 mm
305 in sediments at 1306, 2470, and 3003 mbsl, respectively, while in sediments at 885 mbsl, the OPD was barely 0.1 mm
306 (Table S1; Kraal et al., 2012). The surface (0-5 mm) sediment at 1306 mbsl was not fully oxygenated (OPD of 3 mm),
307 which probably explains the detection in relatively low abundance (ca. 20%) of the anaerobic archaea that thrive in the
308 anoxic sediment from 885 mbsl. The low OPD at 1306 mbsl also explains the low *amoA* gene expression in comparison
309 with the deeper surface sediments (Figs. 5b,d). Overall this indicates the presence of Thaumarchaeota with lower
310 activity in the surface sediments at 1306 mbsl (Fig. 5). Within the Thaumarchaeota MGI group, we also detected
311 changes in the relative abundance of specific OTUs in the surface sediments at 1306, 2470 and 3003 mbsl (Table 5).
312 For example, OTU-2 becomes progressively more abundant with increasing water depth, suggesting that this OTU is
313 favored at the higher oxygen concentrations found in the surface sediment at 3003 mbsl. OTU-4 was closely affiliated

314 with '*Ca. Nitrosopelagicus brevis*', a pelagic MG-I member, which indicates that this DNA is most likely derived from
315 the overlying water column (Table 5), and thus should be considered to represent fossil DNA.

316 High *amoA* gene abundances were detected in the surface sediment at 2470 and 3003 mbsl, while values in the surface
317 of 885 mbsl were approximately three orders of magnitude less. The lack of oxygen in the surface sediments at 885
318 mbsl and in the subsurface sediments, as well as undetectable *amoA* gene transcripts at those depths, suggest that in
319 these cases the *amoA* gene DNA signal is fossil. It is well known that under anoxic conditions DNA of marine pelagic
320 microbes may become preserved in sediments even for periods of thousands of years (Boere et al., 2011; Coolen et al.,
321 2004b). The fossil origin of the Thaumarchaeotal *amoA* gene is supported by the phylogenetic affiliation of the *amoA*
322 gene fragments amplified from the 885 mbsl surface sediment, as those sequences were closely related to *amoA* gene
323 sequences detected in the suspended particulate matter in the subsurface water column (Villanueva et al., 2014), thus
324 suggesting that the detected DNA originated from pelagic Thaumarchaeota present in the subsurface water column, as
325 proposed for the presence of OTU-4 16S rRNA gene sequences in the surface sediment (see earlier).

326 There is a discrepancy between the 16S rRNA gene copy numbers and the *amoA* gene copy numbers within the
327 sediments (Fig. 5). *AmoA* gene copies were consistently lower than the 16S rRNA gene copies, even within sediments
328 that were completely dominated by Thaumarchaeota MG-I. This may be caused by the *amoA* gene primer mismatches
329 and/or the disparity of gene copy numbers within the archaeal genomes (Park et al., 2008).

330 In the anoxic surface sediment at 885 mbsl (within the OMZ), we detected a highly diverse archaeal population
331 composed of MCG, Thermoplasmatales, MBG-B, -D and -E, Woesearchaeota, and MHVG. Archaeal groups such as
332 MCG and MBG-B and E have been previously described in anoxic marine sediments, where they have been suggested
333 to be involved in anaerobic OM degradation (e.g. Biddle et al., 2006; Inagaki et al., 2003; Castelle et al., 2015).
334 Members of the DPANN Woesearchaeota were only present in the surface sediment at 885 mbsl but not in the
335 subsurface anoxic sediments at 885 and 1306 mbsl, suggesting that their presence here is not solely dependent on the
336 absence of oxygen but possibly also on the OM composition and availability in surface and subsurface sediments.
337 Alternatively, the Woesearchaeota 16S rRNA gene signal could also originate from the water column and deposited in
338 the surface sediment at 885 mbsl as fossil DNA as observed for the case of Thaumarchaeota as mentioned above.

339 **Archaeal community composition in the anoxic subsurface sediments**

340 The archaeal diversity in the subsurface sediment (10–12 cm) from both 885 and 1306 mbsl (i.e. dominated by MCG,
341 MBG-B, -D and -E) is similar to that observed in the surface sediment at 885 mbsl. This supports that oxygen
342 availability is an important factor for determining the diversification of archaeal groups (Fig. 1b). MCG, one of the
343 dominant archaeal groups in these sediments, showed substantial differences in the distribution of its subgroups (Table
344 4). All subsurface sediments had a high intra-group diversity of MCG. This is in contrast with the surface sediment at
345 885 and 1306 mbsl where a high relative abundance of the subgroup MCG-15 is detected (Table 4). A recent survey of
346 the ecological niches and substrate preferences of the MCG in estuarine sediments based on genomic data pointed to

347 MCG-6 archaea as degraders of complex extracellular carbohydrate polymers (plant-derived), while subgroups 1, 7, 15
348 and 17 have mainly the potential to degrade detrital proteins (Lazar et al., 2016). Lazar et al. (2016) also described the
349 presence of aminopeptidases coded in the genome bin of MCG-15, suggesting that this subgroup could be specialized in
350 degradation of extracellular peptides in comparison with the other MCG subgroups, which would be restricted to the
351 use of amino acid and oligopeptides. Considering the dominance of the MCG-15 subgroup in the surface sediments
352 analyzed in this study (Table 4), we hypothesize that the proteinaceous OM deposited in the surface sediment, which
353 mainly originates from photosynthate, is still quite undegraded. This would favor the MCG-15 in this niche, fueling its
354 metabolism by the degradation of peptides extracellularly, while in subsurface sediments, other MCG groups such as 2,
355 8 and 14 would be more favored.

356 The archaeal 16S rRNA gene abundance in the subsurface sediments progressively declined with increasing water
357 depth, while the potential activity was similar. This can be due to the expected decrease in the flux of OM being
358 delivered to these anoxic sediments layers attributed to higher degradation of OM in oxygenated bottom waters and the
359 progressively larger oxic zone in the sediments (Lengger et al., 2012; Nierop et al., 2017). This results in lower organic
360 carbon concentrations and a decreased biochemical quality of the OM (Koho et al., 2013; Nierop et al., 2017) to sustain
361 the heterotrophic archaeal population inhabiting the anoxic subsurface sediments. Also the presence or lack of
362 macrofauna in the analyzed sediments would have an effect on the OM composition, sediments within the OMZ are less
363 prone to bioturbation which most likely resulted in higher OM preservation (Koho et al., 2013). Differences in the OM
364 biochemical composition can influence the microbial community composition as was shown recently for North Sea
365 sediments (Oni et al., 2015).

366 **Benthic archaea as potential sources for archaeal IPLs**

367 Archaeal lipids in surface and deeper sediments of the Murray Ridge (Lengger et al., 2012, 2014), as well as in the
368 overlaying water column (Pitcher et al., 2011; Schouten et al., 2012), have been studied earlier. The study by Lengger et
369 al. (2012) was limited to the determination of MH-, DH- and HPH-crenarchaeol with HPLC/ ESI-MS² using a specific
370 selected reaction monitoring method (SRM; Pitcher et al., 2011). A follow-up study of Lengger et al. (2014) reported
371 MH-, DH- and HPH-IPLs with multiple CL-GDGTs. In our study, we expanded the screening for IPLs carrying
372 different polar head groups in combination with multiple CLs using high resolution accurate mass/mass spectrometry
373 (see Table S1). By applying this method, we were able to target a broader range of IPLs in these sediments. This allows
374 a more direct comparison with the archaeal diversity detected by gene-based methods. Note that the study of Lengger et
375 al. (2014) used a different sampling resolution (surface sediment used was 0-2 compared to our 0-0.5 cm) and our
376 results can, therefore, not be directly compared.

377 The fully oxygenated surface sediments showed a dominance of GDGT-0 and crenarchaeol mostly with HPH as IPL-
378 type (Table 2). This is the expected IPL-GDGT signature of Thaumarchaeota as previously observed in pure cultures
379 (Elling et al., 2015, 2017; Pitcher et al., 2010; Qin et al., 2015; Schouten et al., 2008; Sinninghe Damsté et al., 2012).

380 The predominance of the HPH IPL-type in surface (0-2 cm) sediments was previously interpreted as an indication of
381 the presence of an active Thaumarchaeotal population synthesizing membrane lipids *in situ* (Lengger et al., 2012,
382 2014), taking into account the labile nature of sedimentary phospholipids (Harvey et al., 1986; Schouten et al., 2010;
383 Xie et al., 2013). This hypothesis is strongly supported by our data because (i) the archaeal community in the
384 oxygenated surface (0-0.5 cm) sediments is dominated by Thaumarchaeota (Fig. 1) and (ii) the high abundance of
385 thaumarchaeotal *amoA* gene copies and gene transcripts detected in the oxygenated surface sediments. On the other
386 hand, in the anoxic surface sediment at 885 mbsl, crenarchaeol was predominantly present with DH as the predominant
387 IPL-type (Table 2). This is considered to be a fossil signal of Thaumarchaeota deposited from the water column due to a
388 higher preservation potential of glycolipid head groups (as present in DH) as previously suggested (Lengger et al.,
389 2012, 2014). However, Logemann et al. (2011) showed in a 100 day degradation experiment that IPL GDGTs (ether-
390 bound lipids) were hardly degraded in anoxic sediments and, hence, the differences in degradation rates between
391 phospholipid versus glycolipid GDGTs still need to be determined, especially on longer time scales that apply to
392 sediments. Nevertheless, the presence of *amoA* gene sequences in the 885 mbsl surface sediment, which are derived
393 from the deeper water column, as well as the much lower *amoA* gene abundance and lack of *amoA* gene expression
394 (Fig. 5b, d) supports the contention that the crenarchaeol IPLs in the surface sediment at 885 mbsl are predominantly
395 fossil since evidence for active Thaumarchaeota is lacking.

396 The low relative abundance of GDGT-0 IPLs in the surface sediment at 885 mbsl (Table 2) is remarkable. Only MH-
397 GDGT-0 was detected in low relative abundance (0.3 %), whereas any other of the IPL-types with GDGT-0 as CL that
398 were screened for in our study (Table S2; Fig. 1b) was absent. In contrast, Lengger et al. (2012) reported a significant
399 amount of IPL-derived CL-GDGT-0 (i.e. 18.5% of total CL GDGTs) when the head groups of the IPLs are released by
400 acid hydrolyses and the remaining CLs were analyzed in a surface (0-0.5 cm) sediment from the same site. We re-
401 analyzed the IPL-derived CL-GDGT composition in the surface (0-0.5 cm) sediment at 88 mbsl and recovered an
402 identical CL-GDGT distribution as reported by Lengger et al. (2014). The discrepancy between CL and IPL distribution
403 may partly be explained by the underestimation of MH IPLs by our method. However, the difference in response factor
404 for the different IPL types is not sufficient to explain this discrepancy. Therefore, we speculate it is due to the presence
405 of an IPL-type with unknown head groups not included in our analytical window. This unknown IPL GDGT-0 may
406 originate from any of the archaeal groups present in the surface sediment at 885 mbsl, such as MCG,
407 Thermoplasmatales, MBG-B, MBG-E and Euryarchaeota MHVG. Woese archaeota also occur relatively abundant in
408 the surface sediments at 885 mbsl (Fig. 1) but recent studies suggest that their small genomes lack the genes coding for
409 the enzymes of the GDGT biosynthetic pathway (Jahn et al., 2004; Podar et al., 2013; Villanueva et al., 2017; Waters et
410 al., 2003). Therefore, they are not expected to contribute to the IPL-GDGT pool. Ruling out the Woese archaeota as a
411 possible source of IPL-GDGTs, the IPL GDGT-0 with unknown polar head group(s) in the surface sediment at 885
412 mbsl may be attributed to the MCG, which make up 30.5% of the archaeal 16S rRNA gene reads in this sediment. Most

413 of these MCG archaea fall into subgroup MCG-15 (Table 4). Previous studies proposed butanetriol dibiphytanyl
414 glycerol tetraethers (BDGTs) as putative biomarker of the MCG based on the correlation between the presence of these
415 components and MCG in estuarine sediments (Meador et al., 2014). However, we did not detect any IPL BDGTs in the
416 sediments analyzed in our study. Buckles et al. (2013) suggested that members of the MCG and Crenarchaeota group
417 1.2 could be the biological source of IPL GDGT-0 found in the anoxic hypolimnion of a tropical lake. Considering
418 these evidences, it is possible that the unknown IPL GDGT-0 present in the surface sediment at 885 mbsl could be a
419 biomarker for MCG.

420 In subsurface sediments, the IPL GDGT distribution was remarkably different from that detected in the surface
421 oxygenated sediment as higher relative abundances of GDGT-1, 2, 3 and 4 were detected in detriment of GDGT-0,
422 similar to the distribution detected in the surface sediments at 885 mbsl. This may represent new archaeal production in
423 the anoxic sediments, selective preservation of archaeal lipids produced in the water column and surface sediments, or
424 both. The HCP GDGT-0 and two isomers of the DH GDGT-0 (Fig. S2) were detected in the subsurface sediments at
425 885 and 1306 mbsl but not in those from deeper waters (Table 2). Since these IPLs were not detected in the surface
426 sediments, it is likely that they are produced *in situ*. Unfortunately, we only obtained information on the archaeal
427 community composition of the subsurface sediments at shallow water depth, so we cannot compare these with the
428 subsurface sediments from deeper waters that lack these DH moieties, which could have provided a clue towards the
429 archaeal source of these IPLs. An IPL composed of GDGT-0 with a cyclopentanetetraol head group has been
430 previously detected in cultures of the hyperthermophilic crenarchaeal *Sulfolobales* (Langworthy et al., 1974; Sturt et al.,
431 2004). However, members of the *Sulfolobales* were not detected in our 16S rRNA gene amplicon sequencing data. We
432 also detected a high relative abundance of MCG (up to 48.4% relative abundance) in the subsurface sediment at 885 and
433 1306 mbsl (Fig. 1). The diversity of the MCG population in the subsurface sediments was much higher in comparison
434 with the diversity in surface sediments at 885 mbsl as sequences closely related to the MCG subgroups, 2, 8, 10, 14, 5b,
435 15, and 17 were detected both in the 885 mbsl and 1306 mbsl subsurface sediments (Fig. 2). This presence of these
436 different MCG members, likely caused by niche differentiation (see before), may be the origin of the unusual DH-
437 GDGT-0 isomer and the HCP-GDGT-0 IPL that we detected within the subsurface sediments at 885 and 1306 mbsl.

438 CONCLUSIONS

439 By using a combined 16S rRNA gene amplicon sequencing and IPL analysis with high-resolution accurate mass/mass
440 spectrometry we have unraveled the high diversity of benthic archaea harbored in oxygenated and anoxic sediments of
441 the Arabian Sea, as well as widening our detection window of archaeal intact polar lipids. DNA-based analyses
442 revealed a dominance of active benthic *in situ* Thaumarchaeota in those sediment where oxygen was present, which
443 coincided with high relative abundance of the HPH-crenarchaeol previously suggested to be a marker of living
444 Thaumarchaeota. In the anoxic marine sediments analyzed here, members of the MCG, DPANN and Euryarchaeota

445 Thermoplasmatales dominated. We also observed a high diversity within the MCG with a more diverse population in
446 subsurface sediments. Subsurface anoxic sediments had a high relative abundance of IPL GDGT-1, 2, and 3 with DH
447 headgroups, which could either be attributed to fossil signal due to the more recalcitrant nature of the glycosidic bonds
448 or being IPLs synthesized by the archaeal groups detected in those sediments. In addition, IPL GDGT-0 was also
449 detected with a hexose head group on both ends of the core lipid, two hexoses on one end, and a cyclopentanetetraol
450 molecule bound to the core lipid and a hexose attached to it. Members of the DPANN could possibly be ruled out of
451 making those lipids due to the lack of lipid biosynthetic pathway. Dominant archaeal members in those sediments such
452 as the MCG and Thermoplasmatales, could be potential biological sources of these IPLs. To conclude, this combined
453 approach has shed light on the possible biological sources of specific archaeal IPLs and also detected a highly diverse
454 benthic archaeal community.

455 **Acknowledgments**

456 Elda Panoto is thanked for assistance with molecular analyses. We would like to thank the captain and crew of the RV
457 *Pelagia* as well as the cruise leader, technicians and scientists participating in cruise 64PE301. This PASOM cruise was
458 funded by the Earth and Life Science and Research Council (ALW) with financial aid from the Netherlands
459 Organization for Scientific Research (NWO) (grant 817.01.015) to Prof. G.J. Reichart (PI). NIOZ is acknowledged for
460 the studentship of MAB. This research was further supported by the NESSC and SIAM Gravitation Grants
461 (024.002.001 and 024.002.002) from the Dutch Ministry of Education, Culture and Science (OCW) to JSSD.

462 **References**

- 463 Altschul, S. F., Gish, W., Miller, W., Myers, E. W. and Lipman, D. J.: Basic local alignment search tool., *J. Mol. Biol.*,
464 215(3), 403–10, doi:10.1016/S0022-2836(05)80360-2, 1990.
- 465 Biddle, J. F., Lipp, J. S., Lever, M. a, Lloyd, K. G., Sørensen, K. B., Anderson, R., Fredricks, H. F., Elvert, M., Kelly,
466 T. J., Schrag, D. P., Sogin, M. L., Brenchley, J. E., Teske, A., House, C. H. and Hinrichs, K.-U.: Heterotrophic Archaea
467 dominate sedimentary subsurface ecosystems off Peru., *Proc. Natl. Acad. Sci. U. S. A.*, 103(10), 3846–3851,
468 doi:10.1073/pnas.0600035103, 2006.
- 469 Bligh, E. G., Dyer, W. J.: A rapid method of total lipid extraction and Purification, *Can. J. Biochem. Physiol.*, 37, 911–
470 917, doi:10.1139/o59-099., 1959.
- 471 Boere, A. C., Rijpstra, W. I. C., de Lange, G. J., Sinninghe Damsté, J. S. and Coolen, M. J. L.: Preservation potential of
472 ancient plankton DNA in Pleistocene marine sediments, *Geobiology*, 9, 377–393, doi:10.1111/j.1472-
473 4669.2011.00290.x, 2011.
- 474 Buckles, L. K., Villanueva, L., Weijers, J. W. H., Verschuren, D. and Sinninghe Damsté, J. S.: Linking isoprenoidal
475 GDGT membrane lipid distributions with gene abundances of ammonia-oxidizing Thaumarchaeota and uncultured
476 crenarchaeotal groups in the water column of a tropical lake (Lake Challa, East Africa), *Environ. Microbiol.*, 2,
477 doi:10.1111/1462-2920.12118, 2013.
- 478 Caporaso, J. G., Kuczynski, J., Stombaugh, J., Bittinger, K., Bushman, F. D., Costello, E. K., Fierer, N., Peña, A. G.,
479 Goodrich, J. K., Gordon, J. I., Huttley, G. A., Kelley, S. T., Knights, D., Koenig, J. E., Ley, R. E., Lozupone, C. A.,
480 Mcdonald, D., Muegge, B. D., Pirrung, M., Reeder, J., Sevinsky, J. R., Turnbaugh, P. J., Walters, W. A., Widmann, J.,
481 Yatsunencko, T., Zaneveld, J. and Knight, R.: correspondEnce QIIME allows analysis of high- throughput community
482 sequencing data Intensity normalization improves color calling in SOLiD sequencing, *Nat. Publ. Gr.*, 7(5), 335–336,
483 doi:10.1038/nmeth0510-335, 2010.

484 Castelle, C. J., Wrighton, K. C., Thomas, B. C., Hug, L. A., Brown, C. T., Wilkins, M. J., Frischkorn, K. R., Tringe, S.
485 G., Singh, A., Markillie, L. M., Taylor, R. C., Williams, K. H. and Banfield, J. F.: Genomic Expansion of Domain
486 Archaea Highlights Roles for Organisms from New Phyla in Anaerobic Carbon Cycling, *Curr. Biol.*, 25, 1–12,
487 doi:10.1016/j.cub.2015.01.014, 2015.

488 Coolen, M. J. L., Muyzer, G., Rijpstra, W. I. C., Schouten, S., Volkman, J. K. and Sinninghe Damsté, J. S.: Combined
489 DNA and lipid analyses of sediments reveal changes in Holocene haptophyte and diatom populations in an Antarctic
490 lake, *Earth Planet. Sci. Lett.*, 223(1–2), 225–239, doi:10.1016/j.epsl.2004.04.014, 2004a.

491 Coolen, M. J. L., Hopmans, E. C., Rijpstra, W. I. C., Muyzer, G., Schouten, S., Volkman, J. K. and Sinninghe Damsté,
492 J. S.: Evolution of the methane cycle in Ace Lake (Antarctica) during the Holocene: response of methanogens and
493 methanotrophs to environmental change, *Org. Geochem.*, 35(10), 1151–1167, doi:10.1016/j.orggeochem.2004.06.009,
494 2004b.

495 Delong, E. F. and Pace, N. R.: Environmental Diversity of Bacteria and Archaea, *Soc. Syst. Biol.*, 50(4), 470–478,
496 doi:10.1080/10635150118513, 2001.

497 DeLong, E. F., Ying Wu, K., Prézelin, B. B. and Jovine, R. V. M.: High abundance of Archaea in Antarctic marine
498 picoplankton, *Nature*, 371, 695–697, doi:10.1038/371695a0, 1994.

499 Durbin, A. M. and Teske, A.: Sediment-associated microdiversity within the Marine Group I Crenarchaeota, *Environ.*
500 *Microbiol. Rep.*, 2(5), 693–703, doi:10.1111/j.1758-2229.2010.00163.x, 2010.

501 Edgar, R. C.: MUSCLE: Multiple sequence alignment with high accuracy and high throughput, *Nucleic Acids Res.*,
502 32(5), 1792–1797, doi:10.1093/nar/gkh340, 2004.

503 Elling, F. J., Konneke, M., Lipp, J. S., Becker, K. W., Gagen, E. J. and Hinrichs, K. U.: Effects of growth phase on the
504 membrane lipid composition of the thaumarchaeon *Nitrosopumilus maritimus* and their implications for archaeal lipid
505 distributions in the marine environment, *Geochim. Cosmochim. Acta*, 141, 579–597, doi:10.1016/j.gca.2014.07.005,
506 2014.

507 Elling, F. J., Könneke, M., Mußmann, M., Greve, A. and Hinrichs, K.-U.: Influence of temperature, pH, and salinity on
508 membrane lipid composition and TEX86 of marine planktonic thaumarchaeal isolates, *Geochim. Cosmochim. Acta*,
509 171, 238–255, doi:10.1016/j.gca.2015.09.004, 2015.

510 Elling, F. J., Könneke, M., Nicol, G. W., Stieglmeier, M., Bayer, B., Spieck, E., de la Torre, J. R., Becker, K. W.,
511 Thomm, M., Prosser, J. I., Herndl, G. J., Schleper, C. and Hinrichs, K. U.: Chemotaxonomic characterisation of the
512 thaumarchaeal lipidome, *Environ. Microbiol.*, 19(7), 2681–2700, doi:10.1111/1462-2920.13759, 2017.

513 Fillol, M., Auguet, J.-C., Casamayor, E. O. and Borrego, C. M.: Insights in the ecology and evolutionary history of the
514 Miscellaneous Crenarchaeotic Group lineage., *ISME J.*, 1–13, doi:10.1038/ismej.2015.143, 2015.

515 Harvey, H. R., Fallon, R. D. and Patton, J. S.: The effect of organic matter and oxygen on the degradation of bacterial
516 membrane lipids in marine sediments, *Geochim. Cosmochim. Acta*, 50, 795–804, doi:10.1016/0016-7037(86)90355-8,
517 1986.

518 Hopmans, E. C., Schouten, S. and Sinninghe, J. S.: The effect of improved chromatography on GDGT-based
519 palaeoproxies, *Org. Geochem.*, 93, 1–6, doi:10.1016/j.orggeochem.2015.12.006, 2016.

520 Inagaki, F., Suzuki, M., Takai, K., Oida, H., Sakamoto, T., Aoki, K., Nealson, K. H. and Horikoshi, K.: Microbial
521 Communities Associated with Geological Horizons in Coastal Subseafloor Sediments from the Sea of Okhotsk
522 Microbial Communities Associated with Geological Horizons in Coastal Subseafloor Sediments from the Sea of
523 Okhotsk, *Appl. Environ. Microbiol.*, 69(12), 7224–7235, doi:10.1128/AEM.69.12.7224, 2003.

524 Ingalls, A. E., Hugué, C. and Truxal, L. T.: Distribution of intact and core membrane lipids of archaeal glycerol dialkyl
525 glycerol tetraethers among size-fractionated particulate organic matter in Hood Canal, Puget Sound, *Appl. Environ.*
526 *Microbiol.*, 78(5), 1480–1490, doi:10.1128/AEM.07016-11, 2012.

527 Jahn, U., Summons, R., Sturt, H., Grosjean, E. and Huber, H.: Composition of the lipids of *Nanoarchaeum equitans* and
528 their origin from its host *Ignicoccus* sp. strain KIN4/I, *Arch. Microbiol.*, 182(5), 404–413, doi:10.1007/s00203-004-
529 0725-x, 2004.

530 Jorgenson, S. L., Hannisdal, B., Lanzén, A., Baumberg, T., Flesland, K., Fonseca, R., Øvreås, L., Steen, I. H.,
531 Thorseth, I. H., Pedersen, R. B. and Schleper, C.: Correlating microbial community profiles with geochemical data in
532 highly stratified sediments from the Arctic Mid-Ocean Ridge, *Proc. Natl. Acad. Sci.*, 109(42), E2846–E2855,
533 doi:10.1594/PANGAEA.786687, 2012.

534 Karner, M. B., DeLong, E. F. and Karl, D. M.: Archaeal dominance in the mesopelagic zone of the Pacific Ocean,
535 *Nature*, 409(6819), 507–510, doi:10.1038/35054051, 2001.

536 Klindworth, A., Pruesse, E., Schweer, T., Peplies, J., Quast, C., Horn, M. and Glockner, F. O.: Evaluation of general
537 16S ribosomal RNA gene PCR primers for classical and next-generation sequencing-based diversity studies, *Nucleic*

- 538 *Acids Res.*, 41(1), 1–11, doi:10.1093/nar/gks808, 2013.
- 539 Koga, Y. and Morii, H.: Biosynthesis of ether-type polar lipids in archaea and evolutionary considerations., *Microbiol.*
540 *Mol. Biol. Rev.*, 71(1), 97–120, doi:10.1128/MMBR.00033-06, 2007.
- 541 Koho, K. A., Nierop, K. G. J., Moodley, L., Middelburg, J. J., Pozzato, L., Soetaert, K., Van Der Plicht, J. and Reichart,
542 G. J.: Microbial bioavailability regulates organic matter preservation in marine sediments, *Biogeosciences*, 10(2),
543 1131–1141, doi:10.5194/bg-10-1131-2013, 2013.
- 544 Könneke, M., Bernhard, A. E., de la Torre, J. R., Walker, C. B., Waterbury, J. B. and Stahl, D. A.: Isolation of an
545 autotrophic ammonia-oxidizing marine archaeon, *Nature*, 437(22), 543–546, doi:10.1038/nature03911, 2005.
- 546 Kraal, P., Slomp, C. P., Reed, D. C., Reichart, G.-J. and Poulton, S. W.: Sedimentary phosphorus and iron cycling in
547 and below the oxygen minimum zone of the northern Arabian Sea, *Biogeosciences*, 9(7), 2603–2624, doi:10.5194/bg-9-
548 2603-2012, 2012.
- 549 Kubo, K., Lloyd, K. G., F Biddle, J., Amann, R., Teske, A. and Knittel, K.: Archaea of the Miscellaneous
550 Crenarchaeotal Group are abundant, diverse and widespread in marine sediments, *ISME J.*, 6(10), 1949–1965,
551 doi:10.1038/ismej.2012.37, 2012.
- 552 De La Torre, J. R., Walker, C. B., Ingalls, A. E., Könneke, M. and Stahl, D. A.: Cultivation of a thermophilic ammonia
553 oxidizing archaeon synthesizing crenarchaeol, *Environ. Microbiol.*, 10(3), 810–818, doi:10.1111/j.1462-
554 2920.2007.01506.x, 2008.
- 555 Langworthy, T. A., Mayberry, W. R. and Smith, P. F.: Long-chain glycerol diether and polyol dialkyl glycerol triether
556 lipids of *Sulfolobus acidocaldarius*, *J. Bacteriol.*, 119(1), 106–116, 1974.
- 557 Lazar, C. S., Baker, B. J., Seitz, K., Hyde, A. S., Dick, G. J., Hinrichs, K. U. and Teske, A. P.: Genomic evidence for
558 distinct carbon substrate preferences and ecological niches of Bathyarchaeota in estuarine sediments, *Environ.*
559 *Microbiol.*, 18(4), 1200–1211, doi:10.1111/1462-2920.13142, 2016.
- 560 Learman, D. R., Henson, M. W., Thrash, J. C., Temperton, B., Brannock, P. M., Santos, S. R., Mahon, A. R. and
561 Halanych, K. M.: Biogeochemical and microbial variation across 5500 km of Antarctic surface sediment implicates
562 organic matter as a driver of benthic community structure, *Front. Microbiol.*, 7, 1–11, doi:10.3389/fmicb.2016.00284,
563 2016.
- 564 Lengger, S. K., Hopmans, E. C., Reichart, G.-J., Nierop, K. G. J., Sinninghe Damsté, J. S. and Schouten, S.: Intact polar
565 and core glycerol dibiphytanyl glycerol tetraether lipids in the Arabian Sea oxygen minimum zone. Part II: Selective
566 preservation and degradation in sediments and consequences for the TEX86, *Geochim. Cosmochim. Acta*, 98, 244–258,
567 doi:10.1016/j.gca.2012.05.003, 2012.
- 568 Lengger, S. K., Hopmans, E. C., Sinninghe Damsté, J. S. and Schouten, S.: Impact of sedimentary degradation and deep
569 water column production on GDGT abundance and distribution in surface sediments in the Arabian Sea: Implications
570 for the TEX86 paleothermometer, *Geochim. Cosmochim. Acta*, 142, 386–399, doi:10.1016/j.gca.2014.07.013, 2014.
- 571 Lincoln, S. a, Wai, B., Eppley, J. M., Church, M. J., Summons, R. E. and DeLong, E. F.: Planktonic Euryarchaeota are
572 a significant source of archaeal tetraether lipids in the ocean., *Proc. Natl. Acad. Sci. U. S. A.*, 111(27), 9858–63,
573 doi:10.1073/pnas.1409439111, 2014a.
- 574 Lincoln, S. a, Wai, B., Eppley, J. M., Curch, M. J., Summons, R. E. and Delong, E. F.: Reply to Schouten et al. : Marine
575 Group II planktonic Euryarchaeota are significant contributors to tetraether lipids in the ocean, *Proc. Natl. Acad. Sci.*,
576 111(41), 4286, doi:10.1073/pnas.1416736111, 2014b.
- 577 Lipp, J. S. and Hinrichs, K.-U.: Structural diversity and fate of intact polar lipids in marine sediments, *Geochim.*
578 *Cosmochim. Acta*, 73(22), 6816–6833, doi:10.1016/j.gca.2009.08.003, 2009.
- 579 Lipp, J. S., Morono, Y., Inagaki, F. and Hinrichs, K.-U.: Significant contribution of Archaea to extant biomass in
580 marine subsurface sediments., *Nature*, 454(August), 991–994, doi:10.1038/nature07174, 2008.
- 581 Lloyd, K. G., Schreiber, L., Petersen, D. G., Kjeldsen, K. U., Lever, M. a, Steen, A. D., Stepanauskas, R., Richter, M.,
582 Kleindienst, S., Lenk, S., Schramm, A. and Jørgensen, B. B.: Predominant archaea in marine sediments degrade detrital
583 proteins., *Nature*, 496(7444), 215–8, doi:10.1038/nature12033, 2013.
- 584 Logemann, J., Graue, J., Köster, J., Engelen, B., Rullkötter, J. and Cypionka, H.: A laboratory experiment of intact
585 polar lipid degradation in sandy sediments, *Biogeosciences*, 8(9), 2547–2560, doi:10.5194/bg-8-2547-2011, 2011.
- 586 Ludwig, W., Strunk, O., Westram, R., Richter, L., Meier, H., Yadhukumar, Buchner, A., Lai, T., Steppi, S., Jobb, G.,
587 Förster, W., Brettske, I., Gerber, S., Ginhart, A. W., Gross, O., Grumann, S., Hermann, S., Jost, R., König, A., Liss, T.,
588 Lüssmann, R., May, M., Nonhoff, B., Reichel, B., Strehlow, R., Stamatakis, A., Stuckmann, N., Vilbig, A., Lenke, M.,
589 Ludwig, T., Bode, A. and Schleifer, K.-H.: ARB: a software environment for sequence data., *Nucleic Acids Res.*, 32(4),
590 1363–71, doi:10.1093/nar/gkh293, 2004.

- 591 Massana, R., Castresana, J., Balague, V., Guillou, L., Romari, K., Groisillier, A., Valentin, K. and Pedros-Alio, C.:
592 Phylogenetic and Ecological Analysis of Novel Marine Stramenopiles, *Appl. Environ. Microbiol.*, 70(6), 3528–3534,
593 doi:10.1128/AEM.70.6.3528, 2004.
- 594 Meador, T. B., Bowles, M., Lazar, C. S., Zhu, C., Teske, A. and Hinrichs, K.-U.: The archaeal lipidome in estuarine
595 sediment dominated by members of the Miscellaneous Crenarchaeotal Group, *Environ. Microbiol.*, 17(7), 2441–2458,
596 doi:10.1111/1462-2920.12716, 2015.
- 597 Meng, J., Xu, J., Qin, D., He, Y., Xiao, X. and Wang, F.: Genetic and functional properties of uncultivated MCG
598 archaea assessed by metagenome and gene expression analyses, *ISME J.*, 8(3), 650–659, doi:10.1038/ismej.2013.174,
599 2014.
- 600 Moore, E. K., Villanueva, L., Hopmans, E. C., Rijpstra, W. I. C., Mets, A., Dedysh, S. N. and Sinninghe Damsté, J. S.:
601 Abundant trimethylornithine lipids and specific gene sequences are indicative of planctomycete importance at the
602 oxic/anoxic interface in sphagnum-dominated northern wetlands, *Appl. Environ. Microbiol.*, 81(18), 6333–6344,
603 doi:10.1128/AEM.00324-15, 2015.
- 604 Nierop, K. G. J., Reichart, G., Veld, H. and Sinninghe Damsté, J. S.: The influence of oxygen exposure time on the
605 composition of macromolecular organic matter as revealed by surface sediments on the Murray Ridge (Arabian Sea),
606 *Geochim. Cosmochim. Acta*, 206, 40–56, 2017.
- 607 Offre, P., Spang, A. and Schleper, C.: Archaea in Biogeochemical Cycles, *Annu. Rev. Microbiol.*, 437–457,
608 doi:10.1146/annurev-micro-092412-155614, 2013.
- 609 Oni, O. E., Schmidt, F., Miyatake, T., Kasten, S., Witt, M., Hinrichs, K.-U. and Friedrich, M. W.: Microbial
610 Communities and Organic Matter Composition in Surface and Subsurface Sediments of the Helgoland Mud Area,
611 North Sea, *Front. Microbiol.*, 6(November), 1–16, doi:10.3389/fmicb.2015.01290, 2015.
- 612 Park, S.-J., Park, B.-J. and Rhee, S.-K.: Comparative analysis of archaeal 16S rRNA and amoA genes to estimate the
613 abundance and diversity of ammonia-oxidizing archaea in marine sediments, *Extremophiles*, 12(4), 605–615,
614 doi:10.1007/s00792-008-0165-7, 2008.
- 615 Pitcher, A., Rychlik, N., Hopmans, E. C., Spieck, E., Rijpstra, W. I. C., Ossebaar, J., Schouten, S., Wagner, M. and
616 Sinninghe Damsté, J. S.: Crenarchaeol dominates the membrane lipids of *Candidatus Nitrososphaera gargensis*, a
617 thermophilic group I.1b Archaeon, *ISME J.*, 4(4), 542–52, doi:10.1038/ismej.2009.138, 2010.
- 618 Pitcher, A., Villanueva, L., Hopmans, E. C., Schouten, S., Reichart, G.-J. and Sinninghe Damsté, J. S.: Niche
619 segregation of ammonia-oxidizing archaea and anammox bacteria in the Arabian Sea oxygen minimum zone., *ISME J.*,
620 5(12), 1896–904, doi:10.1038/ismej.2011.60, 2011.
- 621 Podar, M., Makarova, K. S., Graham, D. E., Wolf, Y. I., Koonin, E. V and Reysenbach, A.-L.: Insights into archaeal
622 evolution and symbiosis from the genomes of a nanoarchaeon and its inferred crenarchaeal host from Obsidian Pool,
623 Yellowstone National Park., *Biol. Direct*, 8(1), 9, doi:10.1186/1745-6150-8-9, 2013.
- 624 Qin, W., Carlson, L. T., Armbrust, E. V., Devol, A. H., Moffett, J. W., Stahl, D. A. and Ingalls, A. E.: Confounding
625 effects of oxygen and temperature on the TEX₈₆ signature of marine Thaumarchaeota, *Proc. Natl. Acad. Sci.*, 112(35),
626 10979–10984, doi:10.1073/pnas.1501568112, 2015.
- 627 Quast, C., Pruesse, E., Yilmaz, P., Gerken, J., Schweer, T., Yarza, P., Peplies, J. and Glockner, F. O.: The SILVA
628 ribosomal RNA gene database project: improved data processing and web-based tools, *Nucleic Acids Res.*,
629 41(November 2012), D590–D596, doi:10.1093/nar/gks1219, 2013.
- 630 Rinke, C., Schwientek, P., Sczyrba, A., Ivanova, N. N., Anderson, I. J., Cheng, J.-F., Darling, A. E., Malfatti, S., Swan,
631 B. K., Gies, E. a, Dodsworth, J. a, Hedlund, B. P., Tsiamis, G., Sievert, S. M., Liu, W.-T., Eisen, J. a, Hallam, S. J.,
632 Kyrpides, N. C., Stepanauskas, R., Rubin, E. M., Hugenholtz, P. and Woyke, T.: Insights into the phylogeny and coding
633 potential of microbial dark matter., *Nature*, 499(7459), 431–437, doi:10.1038/nature12352, 2013.
- 634 De Rosa, M. and Gambacorta, A.: The lipids of archaeobacteria, *The lipids of archaeobacteria*, 27, 153–175, 1988.
- 635 Rossel, P. E., Lipp, J. S., Fredricks, H. F., Arnds, J., Boetius, A., Elvert, M. and Hinrichs, K. U.: Intact polar lipids of
636 anaerobic methanotrophic archaea and associated bacteria, *Org. Geochem.*, 39(8), 992–999,
637 doi:10.1016/j.orggeochem.2008.02.021, 2008.
- 638 Saitou N, N. M.: The Neighbor-joining Method: A New Method for Reconstructing Phylogenetic Trees', *Mol. Biol.*
639 *Evol.*, 4(4), 406–425, doi:citeulike-article-id:93683, 1987.
- 640 Schleper, C., Jurgens, G. and Jonscheit, M.: Genomic studies of uncultivated archaea, *Nat. Rev. Microbiol.*, 3(6), 479–
641 488, doi:10.1038/nrmicro1159, 2005.
- 642 Schouten, S., Hopmans, E. C., Baas, M., Boumann, H., Standfest, S., Könneke, M., Stahl, D. a. and Sinninghe Damsté,
643 J. S.: Intact membrane lipids of “*Candidatus Nitrosopumilus maritimus*,” a cultivated representative of the cosmopolitan
644 mesophilic group I crenarchaeota, *Appl. Environ. Microbiol.*, 74(8), 2433–2440, doi:10.1128/AEM.01709-07, 2008.

645 Schouten, S., Middelburg, J. J., Hopmans, E. C. and Sinninghe Damsté, J. S.: Fossilization and degradation of intact
646 polar lipids in deep subsurface sediments: A theoretical approach, *Geochim. Cosmochim. Acta*, 74(13), 3806–3814,
647 doi:10.1016/j.gca.2010.03.029, 2010.

648 Schouten, S., Pitcher, A., Hopmans, E. C., Villanueva, L., van Bleijswijk, J. and Sinninghe Damsté, J. S.: Intact polar
649 and core glycerol dibiphytanyl glycerol tetraether lipids in the Arabian Sea oxygen minimum zone: I. Selective
650 preservation and degradation in the water column and consequences for the TEX86, *Geochim. Cosmochim. Acta*, 98,
651 228–243, doi:10.1016/j.gca.2012.05.002, 2012.

652 Schouten, S., Hopmans, E. C. and Sinninghe Damsté, J. S.: The organic geochemistry of glycerol dialkyl glycerol
653 tetraether lipids: A review, *Org. Geochem.*, 54, 19–61, doi:10.1016/j.orggeochem.2012.09.006, 2013.

654 Schouten, S., Villanueva, L., Hopmans, E. C., van der Meer, M. T. J. and Sinninghe Damsté, J. S.: Are Marine Group II
655 Euryarchaeota significant contributors to tetraether lipids in the ocean?, *Proc. Natl. Acad. Sci. U. S. A.*, 111(41), E4285,
656 doi:10.1073/pnas.1416176111, 2014.

657 Schubotz, F., Wakeham, S. G., Lipp, J. S., Fredricks, H. F. and Hinrichs, K.-U.: Detection of microbial biomass by
658 intact polar membrane lipid analysis in the water column and surface sediments of the Black Sea, *Environ. Microbiol.*,
659 11(10), 2720–2734, doi:10.1111/j.1462-2920.2009.01999.x, 2009.

660 Sinninghe Damsté, J. S., Schouten, S., Hopmans, E. C., van Duin, A. C. T. and Geenevasen, J. A. J.: Crenarchaeol: the
661 characteristic core glycerol dibiphytanyl glycerol tetraether membrane lipid of cosmopolitan pelagic crenarchaeota, *J.*
662 *Lipid Res.*, 43, 1641–1651, doi:10.1194/jlr.M200148-JLR200, 2002.

663 Sinninghe Damsté, J. S., Rijpstra, W. I. C., Hopmans, E. C., Jung, M.-Y., Kim, J.-G., Rhee, S.-K., Stieglmeier, M. and
664 Schleper, C.: Intact Polar and Core Glycerol Dibiphytanyl Glycerol Tetraether Lipids of Group I.1a and I.1b
665 Thaumarchaeota in Soil, *Appl. Environ. Microbiol.*, 78(19), 6866–6874, doi:10.1128/AEM.01681-12, 2012.

666 Spang, A., Caceres, E. F. and Ettema, T. J. G.: Genomic exploration of the diversity, ecology, and evolution of the
667 archaeal domain of life, *Science (80-.)*, 357(6351), doi:10.1126/science.aaf3883, 2017.

668 Stetter, K. O., Fiala, G., Huber, G., Huber, R. and Segerer, a: Hyperthermophilic microorganisms, *FEMS Microbiol.*
669 *Rev.*, 75, 117–124, doi:10.1111/j.1574-6968.1990.tb04089.x, 1990.

670 Sturt, H. F., Summons, R. E., Smith, K., Elvert, M. and Hinrichs, K.-U.: Intact polar membrane lipids in prokaryotes
671 and sediments deciphered by high-performance liquid chromatography/electrospray ionization multistage mass
672 spectrometry—new biomarkers for biogeochemistry and microbial ecology, *Rapid Commun. Mass Spectrom.*, 18(6),
673 617–628, doi:10.1002/rcm.1378, 2004.

674 Sugai, A., Sakuma, R., Fukuda, I., Kurosawa, N. and Itoh, Y. H.: The Structure of the Core Polyol of the Ether Lipids
675 from *Sulfolobus acidocaldarius*, *Lipids*, 30(4), 339–344, doi:10.1007/BF02536042, 1995.

676 Teske, A.: Marine deep sediment microbial communities., 2013.

677 Teske, A. and Sørensen, K. B.: Uncultured archaea in deep marine subsurface sediments: have we caught them all?,
678 *ISME J.*, 2(1), 3–18, doi:10.1038/ismej.2007.90, 2008.

679 Villanueva, L., Schouten, S. and Sinninghe Damsté, J. S.: Depth-related distribution of a key gene of the tetraether lipid
680 biosynthetic pathway in marine Thaumarchaeota., *Environ. Microbiol.*, doi:10.1111/1462-2920.12508, 2014.

681 Villanueva, L., Schouten, S. and Sinninghe Damsté, J. S.: Phylogenomic analysis of lipid biosynthetic genes of Archaea
682 shed light on the “lipid divide,” *Environ. Microbiol.*, 19(1), 54–69, doi:10.1111/1462-2920.13361, 2017.

683 Waters, E., Hohn, M. J., Ahel, I., Graham, D. E., Adams, M. D., Barnstead, M., Beeson, K. Y., Bibbs, L., Bolanos, R.,
684 Keller, M., Kretz, K., Lin, X., Mathur, E., Ni, J., Podar, M., Richardson, T., Sutton, G. G., Simon, M., Soll, D., Stetter,
685 K. O., Short, J. M. and Noordewier, M.: The genome of *Nanoarchaeum equitans*: insights into early archaeal evolution
686 and derived parasitism., *Proc. Natl. Acad. Sci. U. S. A.*, 100(22), 12984–8, doi:10.1073/pnas.1735403100, 2003.

687 Xie, S., Lipp, J. S., Wegener, G., Ferdelman, T. G. and Hinrichs, K.-U.: Turnover of microbial lipids in the deep
688 biosphere and growth of benthic archaeal populations, *Proc. Natl. Acad. Sci.*, 110(15), 6010–6014,
689 doi:10.1073/pnas.1218569110, 2013.

690 Yakimov, M. M., Cono, V. La, Smedile, F., DeLuca, T. H., Juárez, S., Ciordia, S., Fernández, M., Albar, J. P., Ferrer,
691 M., Golyshin, P. N. and Giuliano, L.: Contribution of crenarchaeal autotrophic ammonia oxidizers to the dark primary
692 production in Tyrrhenian deep waters (Central Mediterranean Sea)., *ISME J.*, 5(6), 945–61,
693 doi:10.1038/ismej.2010.197, 2011.

694

695

696 **Figure legends**

697 **Fig. 1.** (A) Relative abundances of the IPL-GDGTs (sum of the IPL-types MH, DH and HPH) for the different core
698 GDGTs in the surface (0-0.5 cm) and subsurface sediments (10-12 cm) and (B) the archaeal community composition as
699 revealed by 16S rRNA gene reads (with average abundance above of > 1%) in the surface sediments at 885, 1306,
700 2470, and 3003 mbsl and in the subsurface sediments at 885 and 1306 mbsl.

701 **Fig. 2.** Maximum likelihood phylogenetic tree of the archaeal groups MCG+C3 (modified from Fillol et al., 2015).
702 Extracted OTUs from the Arabian Sea sediments assigned as MCG were inserted in the tree. The number of detected
703 reads per OTU per samples are indicated. Per MCG subgroup the relative abundance is given as detected at the different
704 stations and sediments depths, this is also noted in Table 4. Scale bar represents a 2% sequence dissimilarity.

705 **Fig. 3.** Maximum likelihood phylogenetic tree of MG-I OTUs recovered within the sediment based on the 16S rRNA
706 gene (colored in blue). Sequences from cultured representatives of Thaumarchaeota MG-I are indicated in red.
707 Environmental sequences of MG-I members are indicated in black with their origin specified. The relative abundances
708 of the various OTUs are listed in Table 4. Scale bar represents a 2% sequence dissimilarity.

709 **Fig. 4.** Maximum likelihood phylogenetic tree of *amoA* gene coding sequences recovered from surface (S; 0-0.5 cm)
710 and subsurface (SS; 10-12 cm) sediments (colored in blue) at 885 mbsl, 1306 mbsl and 3003 mbsl (155 clones). *AmoA*
711 gene coding sequences recovered from SPM (colored in orange) at 170 mbsl (28 clones), SPM at 1050 (25 clones)
712 reported by Villanueva et al. (2014). ** indicates *amoA* gene sequences recovered from surface sediments at 3003 mbsl
713 previously reported in Villanueva et al., (2015). Scale bar represents a 2% sequence dissimilarity.

714 **Fig. 5.** Abundance of Thaumarchaeotal 16S rRNA (A,C) and *amoA* (B,D) gene fragment copies per gram of dry weight
715 in the surface sediment (0-0.5 cm) (A,B) and the subsurface sediment (10-12 cm) (C,D). Black bars indicate the amount
716 of DNA 16S rRNA or *amoA* gene fragment copies and the gray bars indicate the RNA (gene transcripts) of 16S rRNA
717 or *amoA* gene fragment copies. Error bars indicate standard deviation based on $n = 3$ experimental replicates.

718

719 **Table 1. Bottom water temperature and oxygen concentration, oxygen penetration depth in the sediment, and**
 720 **TOC content and pore water composition of the surface (0-0.5 cm) sediment^a**

Station (mbsl)	T (°C)	BWO ($\mu\text{mol}\cdot\text{L}^{-1}$)	OPD (mm)	TOC (wt %)	NH ₄ ⁺ (μM)	NO ₂ ⁻ (μM)	NO ₃ ⁻ (μM)	HPO ₄ ²⁻ (μM)
885	10	2.0	0.1	5.6 (\pm 0.2)	2	1.2	1.3	9.2
1306	6.7	14.3	2.9	2.9 (\pm 0.1)	2.6 [*]	0.1 [*]	36.2 [*]	5.6
2470	2.1	63.8	9.8	0.8 (\pm 0.1)	- ^b	-	-	-
3003	1.4	82.9	19	0.7 (\pm 0.1)	55.6	8.3	46.2	3.8

^aData from Kraal et al. (2012) and Lengger et al. (2014)

^bno data available

721

722

723
724

Table 2. Total IPL abundance and heatmap^a of the relative abundance (%) of the detected IPLs and sum (not color coded) per IPL-GDGT in the sediments studied.

Sediment	Depth (mbsl)	GDGT-0						GDGT-1				GDGT-2			
		MH	DH		HCP ^c	HPH	Sum	MH	DH	HPH	Sum	MH	DH	HPH	Sum
			I ^b	II ^b						I ^b			I ^b		
Surface (0-0.5 cm)	885	0.3	ND ^d	ND	ND	ND	0.3	0.1	1.6	ND	1.7	0.1	29.5	ND	29.6
	1306	1.1	ND	ND	ND	36.6	37.6	0.1	1.5	0.2	1.7	ND	15.4	ND	15.4
	2470	0.2	0.1	ND	ND	71.5	71.9	0.0	0.1	0.4	0.5	ND	0.8	ND	0.8
	3003	0.5	0.1	ND	ND	80.3	80.8	ND	0.2	ND	0.2	ND	0.9	ND	0.9
Subsurface (10-12 cm)	885	0.3	ND	7.8	1.6	2.1	11.9	0.1	1.7	0.1	1.9	0.2	27.0	ND	27.1
	1306	2.2	0.9	1.8	0.4	2.1	7.4	0.2	6.7	ND	6.9	0.1	29.7	ND	29.7
	2470	4.3	2.7	ND	ND	18.6	25.6	0.1	5.8	ND	5.9	ND	23.2	ND	23.2
	3003	9.1	3.4	ND	ND	13.0	25.5	0.2	4.3	ND	4.6	ND	21.9	ND	21.9

725

Sediment	Depth (mbsl)	GDGT-3				GDGT-4				Crenarchaeol				IPL abundance [au · g sed dw ⁻¹] ^e	
		MH	DH		HPH	Sum	MH	DH		HPH	Sum	MH	DH		HPH
			I ^b				I ^b				I ^b				
Surface (0-0.5 cm)	885	ND	17.8	ND	17.8	ND	6.1	ND	6.1	1.3	43.1	0.3	44.6	2.7E+09	
	1306	0.0	6.9	ND	6.9	ND	2.7	ND	2.7	1.4	15.5	18.7	35.6	1.2E+10	
	2470	ND	0.2	ND	0.2	ND	0.0	ND	0.0	0.2	0.6	25.8	26.6	2.2E+09	
	3003	ND	0.4	ND	0.4	ND	0.0	ND	0.0	0.4	0.2	17.1	17.6	1.3E+10	
Subsurface (10-12 cm)	885	0.1	15.9	ND	15.9	ND	9.4	ND	9.4	1.1	31.1	1.5	33.8	2.0E+09	
	1306	0.0	14.5	ND	14.5	ND	6.1	ND	6.1	2.7	32.4	0.4	35.5	2.2E+09	
	2470	ND	9.6	ND	9.6	ND	2.9	ND	2.9	3.5	28.3	1.0	32.8	7.8E+08	
	3003	ND	9.7	ND	9.7	ND	5.6	ND	5.6	8.2	23.9	0.6	32.7	1.6E+09	

726

^a Green colors indicate a low relative abundance, red colors indicate a high relative abundance

727

^b DH isomers were detected as a GDGT with a glycosidically-bound hexose moiety on both ends of the core (I) and with one glycosidically-bound dihexose moiety on one end (II).

728

^c HCP is an IPL-type with an ether-bound cyclopentanetetraol moiety on one end and an hexose moiety on the other (previously reported as GDNT; e.g. De Rosa and Gambacorta, 1988; Sturt et al., 2004).

729

^d ND = not detected

730

731

^e Response area of summed IPLs given in au (arbitrary units) per gram of dry weight (dw) sediment.

732

733 **Table 3. Relative abundance of IPL-GDGTs grouped by polar head group^a.**

Sample	Depth (mbsl)	MH	DH	HCP	HPH
Surface (0-0.5 cm)	885	1.7%	98.1%	0.0%	0.3%
	1306	2.6%	42.0%	0.0%	55.4%
	2470	0.5%	1.8%	0.0%	97.7%
	3003	0.8%	1.8%	0.0%	97.4%
Subsurface (10-12 cm)	885	1.8%	92.9%	1.6%	3.7%
	1306	5.2%	91.9%	0.4%	2.5%
	2470	7.9%	72.6%	0.0%	19.6%
	3003	17.6%	68.8%	0.0%	13.6%

734 ^aPolar head group types detected: MH = monohexose, DH = dihexose, both isomers combined, HCP = monohexose and
 735 cyclopentanetetraol, HPH = monohexose and phosphohexose.

736 ^bND = not detected

737

738 **Table 4. Relative abundance (in %) of MCG- and C3-assigned 16S rRNA gene reads relative to total archaeal**
 739 **reads and distribution (in %) of various subgroups for a station within and a station just below the OMZ**

740

Subgroup	885 mbsl		1306 mbsl	
	Surface (0—0.5 cm)	Subsurface (10-12 cm)	Surface (0-0.5 cm)	Subsurface (10-12 cm)
Total	30.5	47.5	1.3	48.8
1		4.6		8.6
2		9.7		10.9
3		<1		2.3
4		<1		
5b		<1		
8	2.3	33.6		10.3
10		13.4		4.0
12	13.6	7.7		8.0
13		1.2		2.3
14	2.3	3.1		10.9
15	77.3	19.6	100	34.3
17	4.5	5.7		8.6

741

742 **Table 5.** Total Thaumarchaeota MG-I 16S rRNA gene reads and distribution per OTU (%) in surface sediments.

	Depth (mbsl)			
	885	1306	2470	3003
Total reads	0	915	1341	1305
OTU ID #1	n.a. ^a	4.3	2.5	3.0
OTU ID #2	n.a.	3.9	8.1	13.6
OTU ID #3	n.a.	43.6	67.6	61.8
OTU ID #4	n.a.	35.1	1.6	0
OTU ID #5	n.a.	3.3	4.7	2.1

743 ^an.a. = not applicable

744

745 **Fig. 1.**

746

747

748

749

750

751

752

753

754

755

756

757

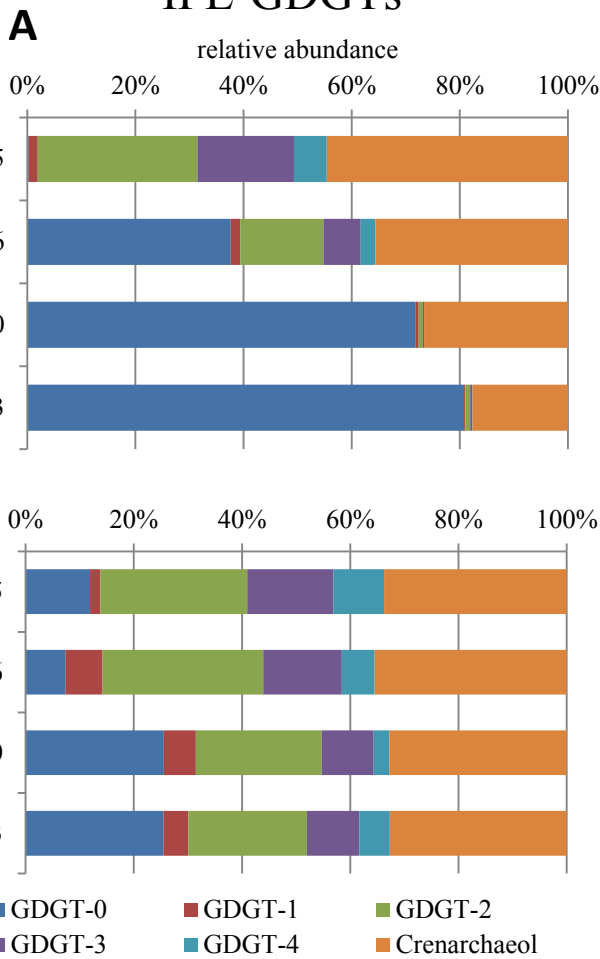
758

759

760

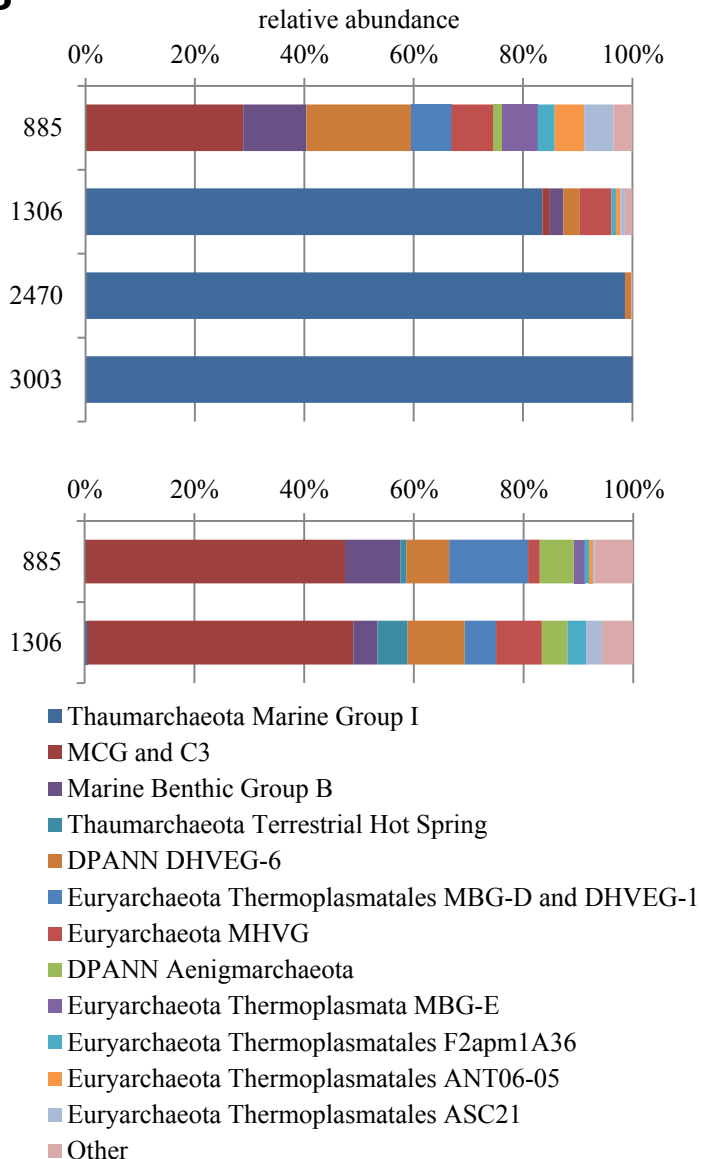
761

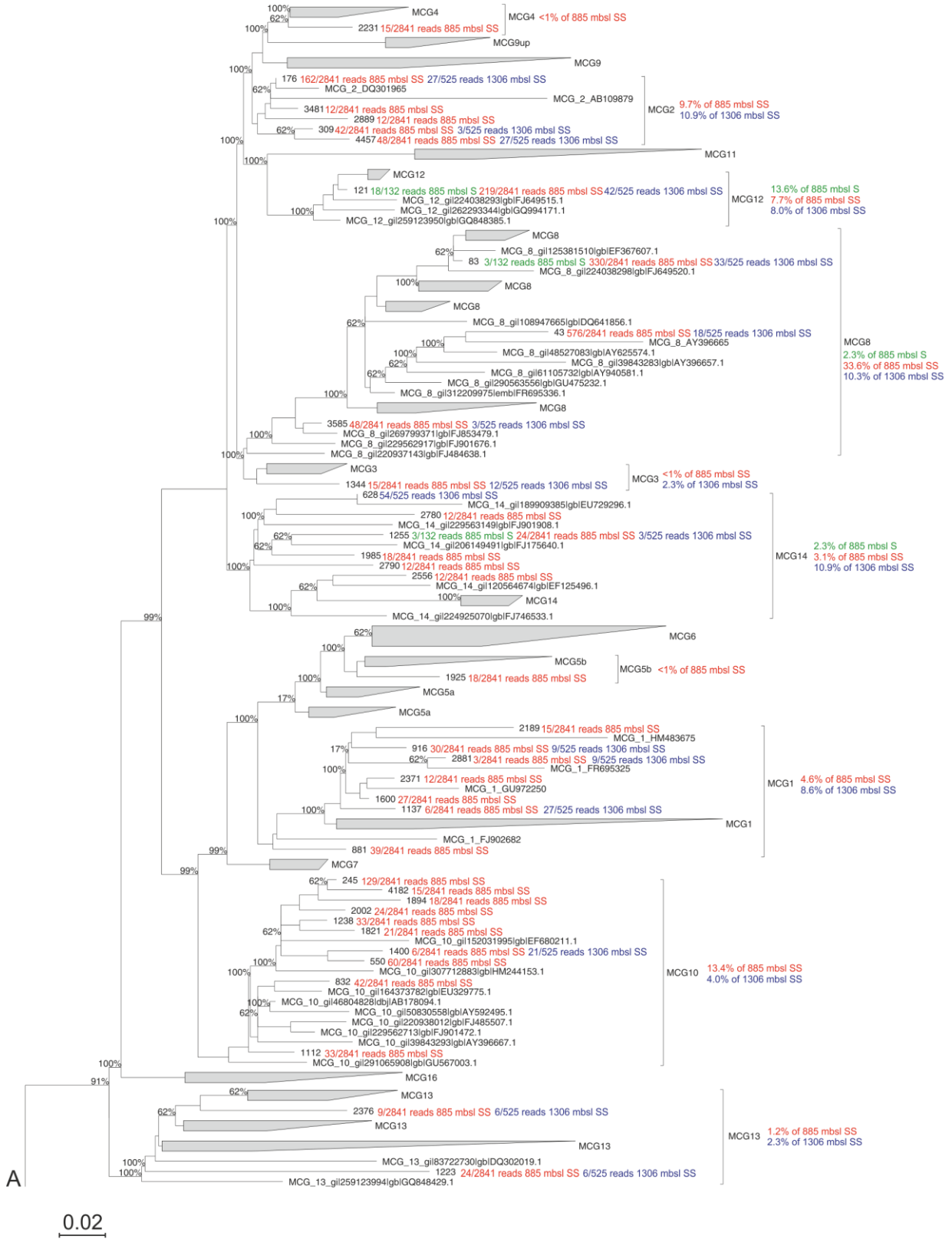
IPL-GDGTs

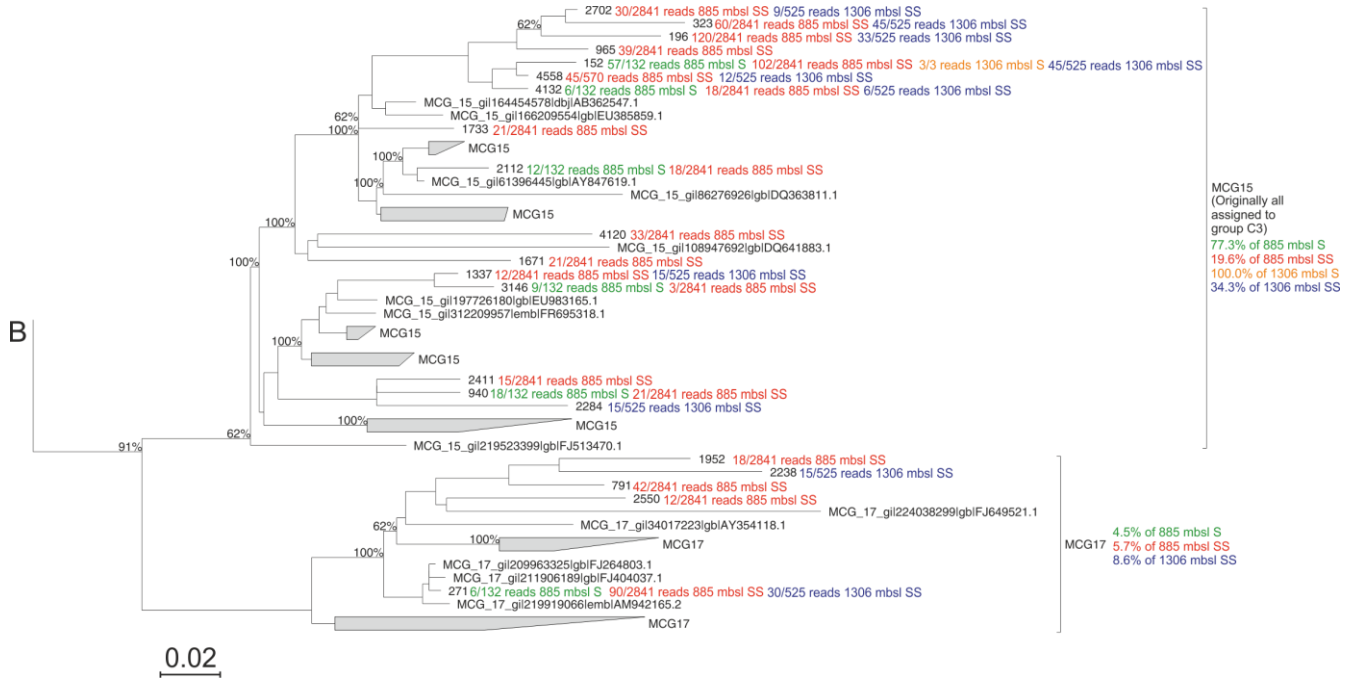


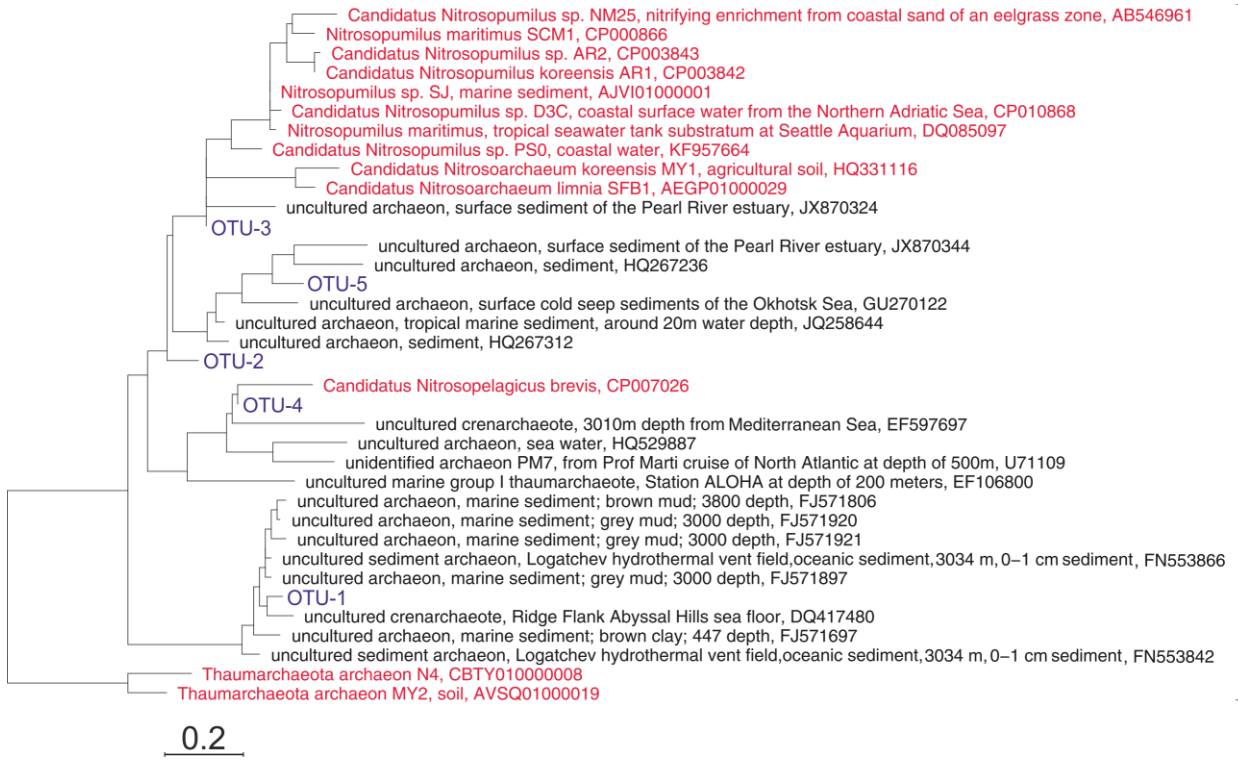
B

Archaeal community composition









Thaumarchaeota MG-I

767
768

769

